# Electronic Supplementary Information

# For

## Ru(II)/Os(II)-based Carbonic Anhydrase Inhibitors as Photodynamic Therapy Photosensitizers for the Treatment of Hypoxic Tumours

Youchao Wang,[a] Pierre Mesdom,[a] Kallol Purkait,[a] Bruno Saubaméa,[b] Pierre Burckel,[c] Philippe Arnoux,[d] Céline Frochot,[d] Kevin Cariou,[a,*] Thibaud Rossel,[e*] and Gilles Gasser,[a,*]

[a] *Chimie ParisTech, PSL University, CNRS, Institute of Chemistry for Life and Health Sciences, Laboratory for Inorganic Chemical Biology, 75005 Paris, France.*

[b] *Cellular and Molecular Imaging Facility, US25 Inserm, UAR3612 CNRS, Faculté de Pharmacie de Paris, Université Paris Cité, F-75006 Paris, France.*

[c] *Institut de Physique du Globe de Paris, Biogéochimie à l'Anthropocène des Eléments et Contaminants Emergents, 75005 Paris, France*

[d] *Université de Lorraine, CNRS, LRGP, F-54000 Nancy, France.*

[e] *University of Neuchâtel, Institute of Chemistry, avenue de Bellevaux 51, 2000 Neuchâtel, Switzerland.*

*kevin.cariou@chimieparistech.psl.eu; thibaud.rossel@unine.ch,*
*gilles.gasser@chimieparistech.psl.eu; Tel: +33 1 85 78 41 51; http://www.gassergroup.com*

# Table of Contents

## 1. Synthesis and Characterization

**General.** Ruthenium trichloride x-hydrate was provided by I$^2$CNS (Zurich); 4,7-diphenyl-1,10-phenanthroline (Bphen), lithium chloride (anhydrous, 99%) and N-Hydroxysuccinimide were obtained from Alfa Aesar. 1,10-phenanthroline, $N_4$-Succinoylsulfanilamide and Ethylenediamine were purchased from Sigma-Aldrich; 4,4'-Dibromo-2,2'-bipyridyl and N,N-Diisopropyléthylamine were sourced from TCI. Potassium hexachloroosmate(IV) was received from Strem Chemicals. All solvents were purchased of analytical or HPLC grade from VWR, and solvents for reactions were of pro analysis (p.a.) grade or distilled prior to their use. Dichlorobis(bathophenanthroline)ruthenium(II) $[Ru(Bphen)_2Cl_2]$ and dichlorobis(bathophenanthroline)osmium(II) $[Os(Bphen)_2Cl_2]$ were synthesized as reported in the literature.[1–3]

**Instruments and Methods.** $^1$H nuclear magnetic resonance ($^1$H NMR) and $^{13}$C nuclear magnetic resonance ($^{13}$C NMR) spectra were determined on a Bruker AV 400 or 500 MHz spectrometer. The chemical shifts, δ, are reported in ppm (parts per million). The residual solvent peaks have been used as internal references. The abbreviations for the peak multiplicities are as follows: s (singlet), d (doublet), t (triplet), m (multiplet), ddd (doublet of doublet of doublets), dt (doublet of triplets (dt). High-resolution ESI mass spectrometry (ESI-

HRMS) spectra were recorded on an LTQ-Orbitrap XL from Thermo Scientific. Analytical HPLC measurement was performed using a 1260 Infinity HPLC System (Agilent Technology) comprising: 2 x Agilent G1361 1260 Prep Pump system with an Agilent G7115A 1260 DAD WR Detector equipped with an Agilent Pursuit XRs 5C18 (100Å, C18 5 μm 250 x 4.6 mm) Column and an Agilent G1364B 1260-FC fraction collector. The solvents (HPLC grade) were acetonitrile (MeCN) (solvent A) and milliQ water (solvent B). The HPLC gradients used are as follow: 0-3 min: isocratic 95% B (5% A); 3-17 min: linear gradient from 95% B (5% A) to 0% B 100% A); 17-23 min: isocratic 0% B (100% A); 23-25 min: linear gradient from 0% B (100% A) to 95% B (5% A). The flow rate was 1 mL/min. Detection was performed at 215 nm, 250 nm, 350 nm, 450 nm, 550 nm, 650 nm with a slit of 4 nm.

3.1 **$[Ru(Bphen)_2(bpy)]^{2+}(2PF_6^-)$ (1).**

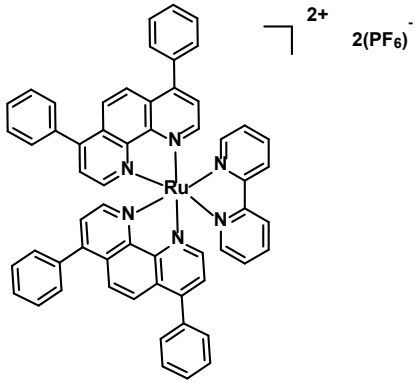


The complex **1** was synthesized in a similar way as reported protocols.[4,5] $Ru(Bphen)_2Cl_2$ (100 mg,0.12 mmol) and bipyridine (20 mg, 0.13 mmol) were suspended in a degassed water/MeOH mixture (1:1 *v/v*) (20 mL) under a $N_2$ atmosphere and refluxed for 15 h. Then the solution was cooled down to room temperature and a saturated aqueous solution of $NH_4PF_6$ was added. The crude solid was purified by chromatography on silica using a system of acetonitrile/potassium nitrate 0.3 M in water (10:1 *v/v*) as eluent. The fractions containing the product were collected and the solvent was removed by rotary evaporation. Then the concentrated product was dissolved in 2 mL of acetonitrile and re-added with a saturated aqueous solution of $NH_4PF_6$, the red-coloured precipitate was washed several times with water, pentane and diethyl ether and dried under vacuum. Yield: 56% (82 mg, 0.068 mmol, $R_f$ = 0.50, acetonitrile/potassium nitrate 0.3 M in water (10:1 *v/v*)). $^1H$ NMR (400 MHz, Acetonitrile-$d_3$) δ 8.61 (dt, *J* = 8.2, 1.1 Hz, 2H), 8.31 (d, *J* = 5.5 Hz, 2H), 8.24 – 8.16 (m, 4H), 8.14 – 8.07 (m, 4H), 7.89 (ddd, *J* = 5.6,

1.5, 0.7 Hz, 2H), 7.76 (d, *J* = 5.5 Hz, 2H), 7.69 – 7.55 (m, 22H), 7.39 (ddd, *J* = 7.6, 5.6, 1.3 Hz, 2H). $^{13}$C NMR (101 MHz, Acetonitrile-$d_3$) δ 158.2, 153.1, 150.1, 150.0, 149.4, 149.2, 138.8, 136.7, 136.6, 130.8, 130.7, 130.6, 130.1, 129.9, 128.4, 127.1, 127.0, 125.2. ESI-HRMS (pos. detection mode): calculated for $C_{58}H_{40}N_6Ru$ $[M\text{-}2PF_6]^{2+}$ m/z 461.1173; found: 461.1171.

**3.2 $[Ru(Bphen)_2(bpy\text{-}Br)_2]^{2+}(2PF_6^-)$ (2).**

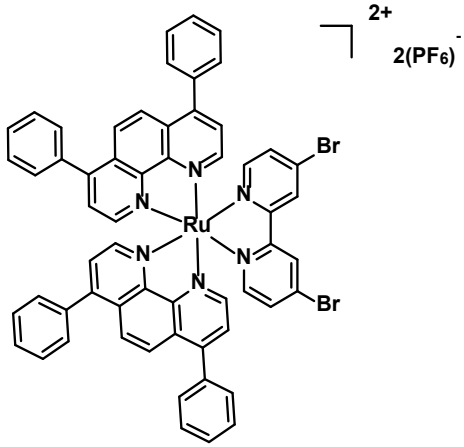


Complex **2** was obtained by a similar synthetic procedure to that for complex **1** using 4,4'-dibromo-2,2'-bipyridine as the ligand. Yield: 60%. ($R_f$ = 0.52, acetonitrile/potassium nitrate 0.3 M in water (10:1 *v/v*)). $^1$H NMR (400 MHz, Acetonitrile-$d_3$) δ 8.85 (d, *J* = 2.0 Hz, 2H), 8.38 (d, *J* = 5.4 Hz, 2H), 8.24 – 8.17 (m, 4H), 8.10 (d, *J* = 5.5 Hz, 4H), 7.80 (d, *J* = 5.5 Hz, 2H), 7.73 (d, *J* = 6.1 Hz, 2H), 7.70 – 7.54 (m, 22H). $^{13}$C NMR (101 MHz, Acetonitrile-$d_3$) δ 158.3, 153.8, 153.4, 153.1, 150.3, 150.2, 149.2, 149.1, 136.7, 136.6, 134.8, 131.8, 130.8, 130.7, 130.6, 130.1, 130.0, 129.9, 129.1, 127.2, 127.0. ESI-HRMS (pos. detection mode): calculated for $C_{58}H_{38}Br_2N_6Ru$ $[M\text{-}2PF_6]^{2+}$ m/z 539.0279; found: 539.0283.

**3.3 $[Ru(Bphen)_2(bpy\text{-}(NH_2)_2)]^{2+}(2PF_6^-)$ (3).**

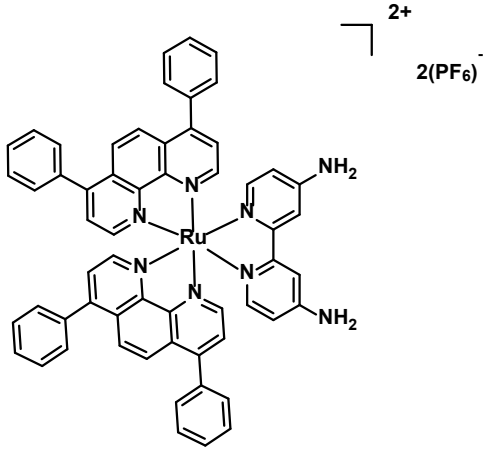

Complex **3** was obtained by a similar synthetic procedure to that for complex **1** using 4,4'-diamino-2,2'-bipyridine as the ligand. Yield: 54%. ($R_f$ = 0.40, acetonitrile/potassium nitrate 0.3 M in water (10:1 *v/v*)). $^1$H NMR (400 MHz, Methanol-$d_4$) δ 8.55 (d, *J* = 5.5 Hz, 2H), 8.27 – 8.11 (m, 6H), 7.88 (d, *J* = 5.5 Hz, 2H), 7.75 – 7.66 (m, 4H), 7.64 – 7.46 (m, 20H), 7.13 (d, *J* = 6.5 Hz, 2H), 6.52 (dd, *J* = 6.5, 2.5 Hz, 2H). $^{13}$C NMR (101 MHz, Methanol-$d_4$) δ 158.6, 157.6, 153.4, 153.1, 151.4, 150.4, 150.0, 149.8, 137.6, 137.5, 131.3, 131.2, 130.8, 130.4, 130.3, 127.7, 127.4, 127.3, 113.3,109.1. ESI-HRMS (pos. detection mode): calculated for $C_{58}H_{42}N_8Ru$ [M-$2PF_6$]$^{2+}$ m/z 476.1282; found: 476.1287. Analytical HPLC: the solvents (HPLC grade) were acetonitrile (MeCN) (solvent A) and milliQ water (solvent B). HPLC gradients used are as follow: 0-3 min: isocratic 95% B (5% A); 3-17 min: linear gradient from 95% B (5% A) to 0% B 100% A); 17-23 min: isocratic 0% B (100% A); 23-25 min: linear gradient from 0% B (100% A) to 95% B (5% A). $T_R$ =11.710 min.

**3.4 [Ru(Bphen)$_2$(bpy-(NHCH$_2$CH$_2$NH$_2$)$_2$)]$^{2+}$(2PF$_6^-$) (4).**

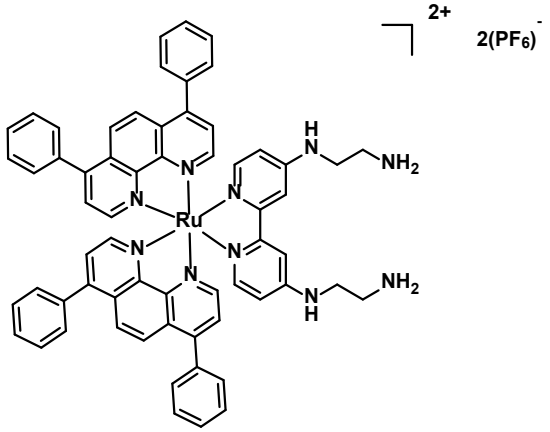


Complex **4** was obtained from microwave reactions between complex **2** and ethylenediamine. **2** (80 mg,0.058 mmol) was dissolved in 1 mL ethylenediamine and the reaction mixture was placed in a microwave tube at 150 °C for 1 h. Then the solution was cooled down to room temperature and a saturated aqueous solution of $NH_4PF_6$ was added. The crude solid was purified by chromatography on silica using a system of acetonitrile/potassium nitrate 0.3 M in water (10:1 *v/v*) as eluent. The fractions containing the product were collected and the solvent was removed by rotary evaporation. Then the concentrated product was dissolved in 2 mL of acetonitrile and re-added with a saturated aqueous solution of $NH_4PF_6$, the red-coloured precipitate was washed several times with water, pentane and diethyl ether and dried under

vacuum. Yield: 81% (58 mg, 0.047 mmol, $R_f$ = 0.17, acetonitrile/potassium nitrate 0.3 M in water (10:1 *v/v*). $^1$H NMR (400 MHz, Methanol-$d_4$) δ 8.56 (dd, *J* = 5.6, 2.0 Hz, 2H), 8.26 – 8.08 (m, 6H), 7.91 – 7.81 (m, 2H), 7.75 – 7.64 (m, 6H), 7.64 – 7.39 (m, 18H), 7.24 (d, *J* = 6.5 Hz, 2H), 6.61 (dd, *J* = 6.6, 2.5 Hz, 2H), 3.63 (t, *J* = 6.1 Hz, 4H), 3.20 (t, *J* = 6.1 Hz, 4H). $^{13}$C NMR (101 MHz, Methanol-$d_4$) δ 158.2, 156.1, 153.4, 151.5, 150.7, 149.9, 137.6, 137.5, 131.3, 131.2, 130.7, 130.4, 130.3, 127.7, 127.4, 43.3, 37.4. ESI-HRMS (pos. detection mode): calculated for $C_{62}H_{52}N_{10}Ru$ $[M\text{-}2PF_6]^{2+}$ m/z 519.1704; found: 519.1705.

The complex **5** and complex **6** were synthesized in the similar way as reported protocols.[6] Complex **5** and complex **6** were obtained by the same synthetic procedure: $N_4$-Succinoylsulfanilamide (22 mg, 0.08 mmol), EDC (12 mg, 0.08 mmol) and NHS (9 mg, 0.08 mmol) was dissolved in 5 mL DMF for the activation of carboxylic acid for 1 h. Then the mixture of complex **4** (50 mg, 0.04 mmol) and DIPEA (5 mg, 0.04 mmol) was added and stirred in room temperature for 48 h. The reaction solution was evaporated to dryness, and then extracted through the mixture solvent ($CH_2Cl_2/H_2O$) for three times. The crude product was purified by chromatography on silica using a system of acetonitrile/potassium nitrate 0.3 M in water (10:1 *v/v*) as eluent to obtain **5** and **6**. The fractions containing the two product were collected and the solvent was removed by rotary evaporation. Then the concentrated product was dissolved in 2 mL of acetonitrile and a saturated aqueous solution of $NH_4PF_6$ was added, the red-coloured precipitate was washed several times with water, pentane and diethyl ether and dried under vacuum.

**3.5 $[Ru(Bphen)_2(bpy\text{-}(NHCH_2CH_2NH_2)_2\text{-}L)]^{2+}(2PF_6^-)$.(L= $N_4$-Succinoylsulfanilamide) (5).**

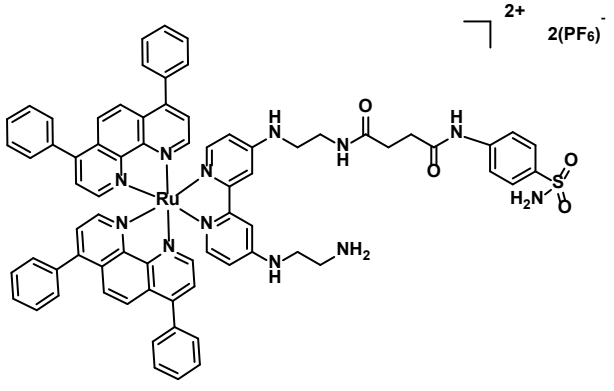

Yield: 25% (16 mg, 0.010 mmol, $R_f$ = 0.21, acetonitrile/potassium nitrate 0.3 M in water (10:1 *v/v*)). $^1$H NMR (500 MHz, Methanol-$d_4$) δ 8.59 (dd, *J* = 12.8, 5.5 Hz, 2H), 8.33 – 8.15 (m, 6H), 7.98 – 7.82 (m, 2H), 7.71 (ddt, *J* = 9.3, 7.9, 1.5 Hz, 6H), 7.67 – 7.51 (m, 22H), 7.20 (dd, *J* = 34.0, 6.6 Hz, 2H), 6.69 – 6.52 (m, 2H), 3.71 – 3.66 (m, 2H), 3.50 – 3.38 (m, 4H), 3.19 (q, *J* = 7.9, 7.1 Hz, 2H), 2.69 (td, *J* = 6.7, 2.5 Hz, 2H), 2.52 (t, *J* = 6.6 Hz, 2H). $^{13}$C NMR (126 MHz, Methanol-$d_4$) δ 175.5, 173.2, 156.8, 156.3, 153.3, 150.4, 149.9, 143.3, 139.5, 137.5, 137.4, 131.3, 131.2, 130.9, 130.8, 130.4, 130.3, 128.2, 127.6, 127.5, 120.4, 42.9, 41.0, 38.7, 32.8, 32.0, 30.9. ESI-HRMS (pos. detection mode): calculated for $C_{72}H_{62}N_{12}O_4RuS$ $[M\text{-}2PF_6]^{2+}$ m/z 646.1885; found: 646.1890. Analytical HPLC: the solvents (HPLC grade) were acetonitrile (MeCN) (solvent A) and milliQ water (solvent B). HPLC gradients used are as follow: 0-3 min: isocratic 95% B (5% A); 3-17 min: linear gradient from 95% B (5% A) to 0% B 100% A); 17-23 min: isocratic 0% B (100% A); 23-25 min: linear gradient from 0% B (100% A) to 95% B (5% A). $T_R$ =11.465 min.

**3.6 $[Ru(Bphen)_2(bpy\text{-}(NHCH_2CH_2NH_2)_2\text{-}L_2)]^{2+}(2PF_6^-)$.(L= N$_4$-Succinoylsulfanilamide) (6).**

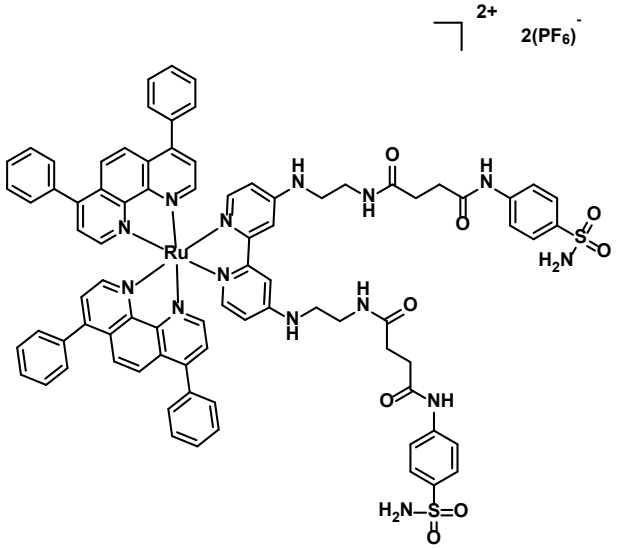


Yield: 9 %. ($R_f$ = 0.38, acetonitrile/potassium nitrate 0.3 M in water (10:1 *v/v*)). $^1$H NMR (400 MHz, Methanol-$d_4$) δ 8.57 (d, *J* = 5.5 Hz, 2H), 8.29 – 8.12 (m, 6H), 7.86 (d, *J* = 5.5 Hz, 2H), 7.77 – 7.67 (m, 6H), 7.65 – 7.46 (m, 26H), 7.14 (d, *J* = 6.6 Hz, 2H), 6.49 (dd, *J* = 6.7, 2.5 Hz, 2H), 3.40 (s, 8H), 2.68 (td, *J* = 6.4, 1.9 Hz, 4H), 2.50 (t, *J* = 6.6 Hz, 4H). $^{13}$C NMR (101 MHz, Methanol-$d_4$) δ 176.1, 173.3, 156.8, 153.3, 150.5, 149.9, 143.7, 139.5, 137.6, 137.5, 131.3, 131.2, 130.9, 130.4, 128.3, 127.7, 127.5, 120.0, 43.4, 39.8, 32.8, 31.3. ESI-HRMS (pos.

detection mode): calculated for $C_{82}H_{72}N_{14}O_8RuS_2$ $[M\text{-}2PF_6]^{2+}$ m/z 773.2026; found: 773.2076. Analytical HPLC: the solvents (HPLC grade) were acetonitrile (MeCN) (solvent A) and milliQ water (solvent B). HPLC gradients used are as follow: 0-3 min: isocratic 95% B (5% A); 3-17 min: linear gradient from 95% B (5% A) to 0% B 100% A); 17-23 min: isocratic 0% B (100% A); 23-25 min: linear gradient from 0% B (100% A) to 95% B (5% A). $T_R$ =11.683 min.

**$PF_6^-$ counter ion exchange**: The $PF6^-$ salt were converted in quantitative yield to its corresponding $Cl^-$ salt using Amberlite IRA-410 with MeOH as the eluent. Full removal of the $PF_6$ anions was controlled by $^{19}F$ NMR (see**Figure S 39**).

### 3.7 $[Os(Bphen)_2(bpy)]^{2+}(2PF_6^-)$ (7).

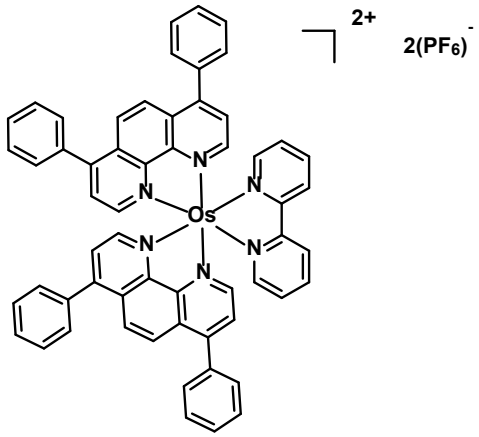


The complex **7** was synthesized in the similar way as reported protocols.[4,5] $Os(Bphen)_2Cl_2$ (200 mg,0.21 mmol) and bipyridine (36 mg, 0.23 mmol) were suspended in ethylene glycol (5 mL) under an inert atmosphere and refluxed for 8 h. Then the solution was cooled down to room temperature and a saturated aqueous solution of $NH_4PF_6$ was added. The crude solid was purified by chromatography on silica using a system of acetonitrile/potassium nitrate 0.3 M in water (10:1 *v/v*) as eluent. The fractions containing the product were collected and the solvent was removed by rotary evaporation. Then the concentrated product was dissolved in 2 mL of methanol and re-added with a saturated aqueous solution of $NH_4PF_6$, the brown-colored precipitate was washed several times with water, pentane and diethyl ether and dried under vacuum. Yield: 42 % (119 mg, 0.091 mmol, $R_f$ = 0.48, acetonitrile/potassium nitrate 0.3 M in water (10:1 *v/v*)). $^1$H NMR (400 MHz, Acetonitrile-$d_3$) δ 8.58 (dt, *J* = 8.3, 1.1 Hz, 2H), 8.26 – 8.14 (m, 6H), 8.03 (d, *J* = 5.6 Hz, 2H), 7.89 (td, *J* = 7.9, 1.4 Hz, 2H), 7.79 (ddd, *J* = 5.8, 1.4, 0.7 Hz, 2H), 7.69 (d, *J* = 5.6 Hz, 2H), 7.66 – 7.52 (m, 24H), 7.29 (ddd, *J* = 7.3, 5.7, 1.3 Hz, 2H). $^{13}$C NMR (101 MHz, Acetonitrile-$d_3$) δ 160.2, 152.8, 152.5, 152.3, 151.6, 151.5, 151.3, 149.8, 149.7, 138.2, 136.4, 131.0, 131.0, 130.6, 130.2, 130.1, 130.0, 128.9, 127.3, 127.2, 125.4. ESI-HRMS (pos. detection mode): calculated for $C_{58}H_{40}N_6Os$ $[M\text{-}2PF_6]^{2+}$ m/z 506.1459; found: 506.1460.

**3.8 $[Os(Bphen)_2(bpy\text{-}Br_2)]^{2+}(2PF_6^-)$ (8).**

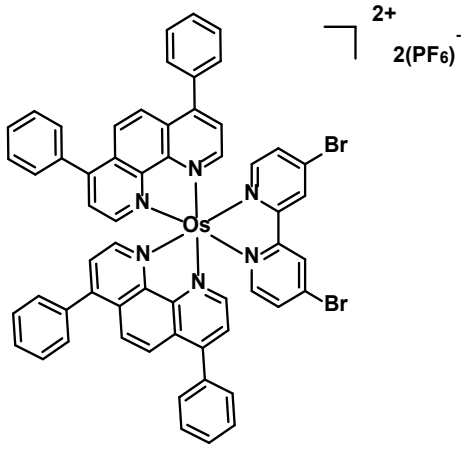


Complex **8** was obtained by a similar synthetic procedure to that for complex **7** using 4,4'-dibromo-2,2'-bipyridine as the ligand. Yield: 49%. ($R_f$ = 0.53, acetonitrile/potassium nitrate 0.3 M in water (10:1 *v/v*)). $^1$H NMR (400 MHz, Acetonitrile-$d_3$) δ 8.79 (d, *J* = 2.1 Hz, 2H), 8.26 – 8.17 (m, 6H), 7.99 – 7.94 (m, 2H), 7.72 (d, *J* = 5.6 Hz, 2H), 7.68 – 7.57 (m, 22H), 7.52 (d, *J* = 5.7 Hz, 2H), 7.45 (dd, *J* = 6.3, 2.1 Hz, 2H). $^{13}$C NMR (101 MHz, Acetonitrile-$d_3$) δ 161.2, 153.0, 152.9, 152.4, 151.3, 151.0, 150.1, 136.4, 136.2, 133.5, 132.3, 131.0, 130.9, 130.6, 130.1, 130.0, 129.2, 127.2, 127.1. 126.9. ESI-HRMS (pos. detection mode): calculated for $C_{58}H_{38}Br_2N_6Os$ $[M\text{-}2PF_6]^{2+}$ m/z 584.0549; found: 584.0542.

**3.9 $[Os(Bphen)_2(bpy\text{-}(NH_2)_2)]^{2+}(2PF_6^-)$ (9).**

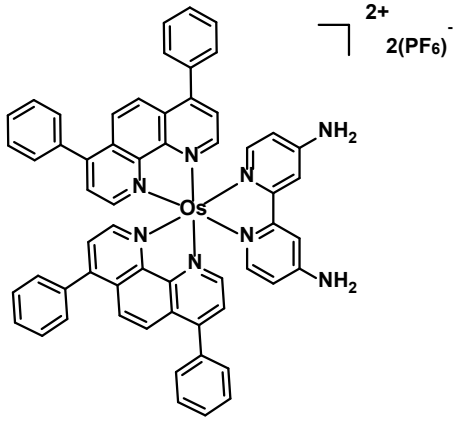


Complex **9** was obtained by a similar synthetic procedure to that for complex **7** using 4,4'-diamino-2,2'-bipyridine as the ligand. Yield: 47%. ($R_f$ = 0.42, acetonitrile/potassium nitrate 0.3 M in water (10:1 *v/v*)). $^1$H NMR (500 MHz, Methanol-$d_4$) δ 8.48 (d, *J* = 5.7 Hz, 2H), 8.29 – 8.21 (m, 4H), 8.05 (d, *J* = 5.7 Hz, 2H), 7.83 (d, *J* = 5.6 Hz, 2H), 7.73 – 7.69 (m, 4H), 7.66 – 7.45 (m, 22H), 7.01 (d, *J* = 6.6 Hz, 2H), 6.49 (dd, *J* = 6.6, 2.5 Hz, 2H).$^{13}$C NMR (126 MHz,

Methanol-$d_4$) δ160.0, 157.6, 153.6, 153.4, 153.1, 152.6, 150.9, 149.8, 137.6, 137.5, 132.0, 131.8, 131.1, 130.9, 130.7, 130.6, 128.2, 128.1, 128.0, 127.8, 113.6, 109.6. ESI-HRMS (pos. detection mode): calculated for $C_{58}H_{42}N_8Os$ $[M\text{-}2PF_6]^{2+}$ m/z 521.1568; found: 521.1566. Analytical HPLC: the solvents (HPLC grade) were acetonitrile (MeCN) (solvent A) and milliQ water (solvent B). The HPLC gradients used are as follow: 0-3 min: isocratic 95% B (5% A); 3-17 min: linear gradient from 95% B (5% A) to 0% B 100% A); 17-23 min: isocratic 0% B (100% A); 23-25 min: linear gradient from 0% B (100% A) to 95% B (5% A).) $T_R$ =11.720 min.

**3.10 $[Os(Bphen)_2(bpy\text{-}(NHCH_2CH_2NH_2)_2)]^{2+}(2PF_6^-)$ (10).**

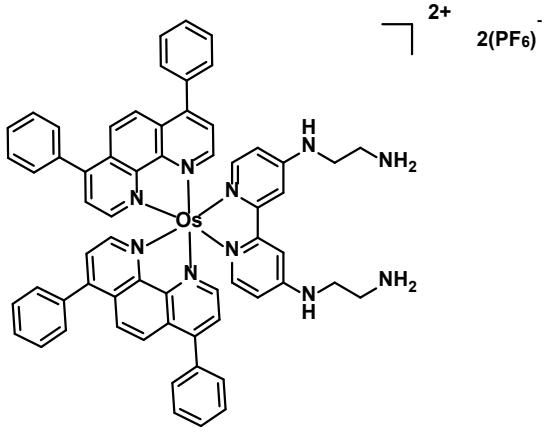


Complex **10** was obtained by a similar synthetic procedure to that for complex **4**. Yield: 75% ($R_f$ = 0.19, acetonitrile/potassium nitrate 0.3 M in water (10:1 *v/v*)). $^1$H NMR δ 8.48 (dd, *J* = 5.6, 3.2 Hz, 2H), 8.24 – 8.10 (m,4H), 8.05 (dd, *J* = 5.7, 3.7 Hz, 2H), 7.78 (dd, *J* = 9.3, 5.6 Hz, 2H), 7.75 – 7.64 (m, 6H), 7.62 – 7.34 (m, 18H), 7.12 (dd, *J* = 6.7, 1.9 Hz, 2H), 6.57 (dd, *J* = 6.7, 2.3 Hz, 2H), 3.67 (t, *J* = 6.3 Hz, 4H), 3.21 (t, *J* = 6.2 Hz, 4H). $^{13}$C NMR (126 MHz, Methanol-$d_4$) δ 159.9, 155.7, 153.1, 153.0, 152.6, 152.5, 150.6, 149.3, 137.2, 131.6, 131.4, 130.7, 130.6, 130.5, 130.4, 130.3, 130.2, 127.9, 127.5, 127.4, 40.9, 37.8. ESI-HRMS (pos. detection mode): calculated for $C_{62}H_{52}N_{10}Os$ $[M\text{-}2PF_6]^{2+}$ m/z 564.1999; found: 564.1990.

Complexes **11** and **12** were obtained by the same synthetic procedure and separated by chromatography in an identical manner as for complexes **5** and **6**.

### 3.11 $[Os(Bphen)_2(bpy\text{-}(NHCH_2CH_2NH_2)_2\text{-}L)]^{2+}(2PF_6^-)$.(L= $N_4$-Succinoylsulfanilamide) (11).

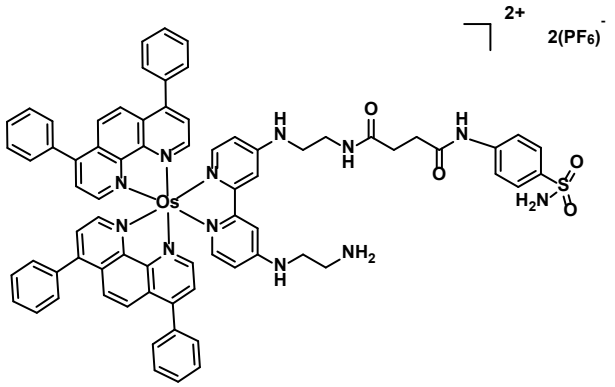


Yield: 18 % ($R_f$ = 0.23, acetonitrile/potassium nitrate 0.3 M in water (10:1 *v/v*)). $^1$H NMR (500 MHz, Methanol-$d_4$) δ 8.52 (dd, *J* = 13.6, 5.6 Hz, 2H), 8.31 – 8.19 (m, 4H), 8.08 (d, *J* = 5.7 Hz, 2H), 7.88 – 7.78 (m, 4H), 7.70 (td, *J* = 8.2, 1.3 Hz, 4H), 7.66 – 7.51 (m, 20H), 7.49 (dd, *J* = 5.7, 3.4 Hz, 2H), 7.07 (dd, *J* = 16.8, 6.7 Hz, 2H), 6.52 (td, *J* = 6.5, 2.6 Hz, 2H), 3.68 (td, *J* = 7.0, 6.5, 3.7 Hz, 2H), 3.56 – 3.34 (m, 4H), 3.26 – 3.16 (m, 2H), 2.67 (td, *J* = 6.9, 4.0 Hz, 2H), 2.51 (t, *J* = 6.8 Hz, 2H). $^{13}$C NMR (126 MHz, Methanol-$d_4$) δ176.7, 173.0, 156.8, 152.6, 149.2, 143.9, 139.6, 137.2, 132.2, 131.7, 131.4, 130.8, 130.3, 127.8, 127.5, 120.4, 42.9, 40.6, 39.6, 33.1, 32.1, 30.8. ESI-HRMS (pos. detection mode): calculated for $C_{72}H_{62}N_{12}O_4OsS$ $[M\text{-}2PF_6]^{2+}$ m/z 691.2174; found: 691.2171. Analytical HPLC: the solvents (HPLC grade) were acetonitrile (MeCN) (solvent A) and milliQ water (solvent B). The HPLC gradients used are as follow: 0-3 min: isocratic 95% B (5% A); 3-17 min: linear gradient from 95% B (5% A) to 0% B 100% A); 17-23 min: isocratic 0% B (100% A); 23-25 min: linear gradient from 0% B (100% A) to 95% B (5% A). $T_R$ = 11.552 min.

**3.12 $[Os(Bphen)_2(bpy\text{-}(NHCH_2CH_2NH_2)_2\text{-}L_2)]^{2+}(2PF_6^-)$.(L= $N_4$-Succinoylsulfanilamide) (12).**

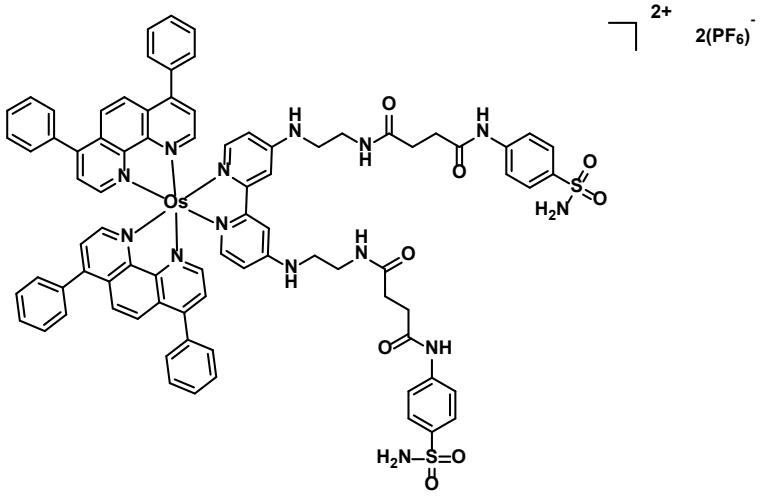


Yield: 13 %. ($R_f$ = 0.40, acetonitrile/potassium nitrate 0.3 M in water (10:1 *v/v*)). $^1$H NMR (400 MHz, Methanol-$d_4$) δ 8.40 (d, *J* = 5.7 Hz, 2H), 8.21 – 8.06 (m, 4H), 7.95 (d, *J* = 5.6 Hz, 2H), 7.68 (d, *J* = 5.7 Hz, 2H), 7.61 – 7.56 (m, 4H), 7.56 – 7.41 (m, 26H), 7.41 – 7.36 (m, 2H), 6.92 (d, *J* = 6.7 Hz, 2H), 6.35 (dd, *J* = 6.7, 2.5 Hz, 2H), 3.31 (d, *J* = 15.2 Hz, 8H), 2.58 (td, *J* = 6.5, 6.1, 2.3 Hz, 4H), 2.40 (t, *J* = 6.6 Hz, 4H). $^{13}$C NMR (101 MHz, Methanol-$d_4$) δ176.1, 173.7, 157.2, 154.2, 153.4, 153.2, 152.9, 149.9, 149.8, 144.1, 139.9, 137.7, 132.1, 131.9, 131.3, 131.0, 130.8, 128.7, 128.4, 128.2, 128.0, 120.8, 45.61, 40.71, 33.24, 32.07. ESI-HRMS (pos. detection mode): calculated for $C_{82}H_{72}N_{14}O_8OsS_2$ $[M\text{-}2PF_6]^{2+}$ m/z 818.2351; found: 818.2354. Analytical HPLC: the solvents (HPLC grade) were acetonitrile (MeCN) (solvent A) and milliQ water (solvent B). The HPLC gradients used are as follow: 0-3 min: isocratic 95% B (5% A); 3-17 min: linear gradient from 95% B (5% A) to 0% B 100% A); 17-23 min: isocratic 0% B (100% A); 23-25 min: linear gradient from 0% B (100% A) to 95% B (5% A). $T_R$ =11.652 min.

**$PF_6^-$ counter ion exchange**: The $PF6^-$ salt were converted in quantitative yield to its corresponding $Cl^-$ salt using Amberlite IRA-410 with MeOH as the eluent. Full removal of the $PF_6$ anions was controlled by $^{19}$F NMR (see**Figure S 41**).

## 2. Spectroscopic measurements

UV-Vis spectra were recorded on Cary 4000 UV-Vis spectrometer (Agilent) and in 96 well plates with BioTeck or with a Varian Cary 8454" UV/Visible spectrophotometer and quartz cuvettes (width 1 cm); Fluorescence spectra were measured by a Horiba Fluorolog Spectrofluorometers.

## 3. Fluorescence quantum yield and Singlet oxygen production measurement

The fluorescence was measured by the UV-Visible detector via the SPEX dual network emission monochromator (1200 lines / mm blasé at 500 nm). Singlet oxygen production was measured with an infrared detector InGaAs (800 - 1550 nm) via the dual network emission monochromator SPEX (600 lines / mm blasé at 1 μm). All spectra were measured using 4-sided quartz cells. $Ru(bpy)_3$ in acetonitrile was choosen as standard for both fluorescence and singlet oxygen quantum yield determination. Fluorescence quantum yield of $Ru(bpy)_3$ in acetonitrile is evaluated at 0.077[7]. Singlet oxygen quantum yield of $Ru(bpy)_3$ in acetonitrile is evaluated at 0.77[8].

Time-resolved experiments were performed using for excitation: a pulsed laser diode emitting at 407 nm (LDH-P-C-400M, FWHM < 70 ps, 1 MHz) coupled with a driver PDL 800-D (both PicoQuant GmbH, BERLIN, Germany) and for detection: an avalanche photodiode SPCM-AQR-15 (EG & G, VAUDREUIL, Canada) coupled with a 650 nm long-wave pass filter as detection system. The acquisition was performed by a PicoHarp 300 module with a 4 channels router PHR-800 (both PicoQuant GmbH, BERLIN, Germany). The fluorescence decays were recorded using the single photon counting method. Data were collected up to 1000 counts accumulated in the maximum channel and analyzed using Time Correlated Single Photon Counting (TCSPC) software Fluofit (PicoQuant GmbH, BERLIN, Germany) based on iterative reconvolution using a Levensberg-Marquandt algoritm, enabling the obtention of multi-exponential profiles.

## 4. Octanol/water partition coefficient (log $P_{o/w}$) measurements

Octanol/water partition coefficients (log $P_{o/w}$) were determined at room temperature following a reported method.[9,10] Octanol (1 mL) and PBS (1 mL) were mixed with each other by continuous shaking at room temperature for 24 h. Then examined complexes (50 μM) were dissolved in 1 mL octanol, and the same volume of PBS was added. The mixture was continue agitated for another 24 h, the two layers were separated after settle down. The concentrations of the complex in two phases were measured by UV-Vis spectrum.

## 5. Particles size tested by dynamic light scattering (DLS)

Hydrodynamic diameters ($D_h$) of the particles and their size distributions in solution (PBS supplemented with 10% FBS) were measured at 25 °C by dynamic light scattering (DLS, Malvern Zetasizer 3000HS, UK) with a 633 nm laser. All measurements were performed with a 90° scattering angle. The sample solution (10 μM, 1%DMSO) in the scattering cell was equilibrated for 2 min before measurements.

## 6. Binding affinity for the inhibition of hCA II

A competitive displacement assay was performed according to the procedure previously described by Zambel.[11] The stock solutions used were HEPES buffer (0.01 M, pH 7.4), ligand stock solution (250 μM, 125 μM, 62.5 μM) in HEPES buffer (0.01 M, pH = 7.4), DNSA (0.1 M in DMSO) and hCA II Wt stock (0.1 M) in HEPES buffer (0.01 M, pH 7.4).

$$r = \frac{1}{1 + (K_{DNSA}/DNSA)(1 + [ligand]/K(ligand))} \quad \text{(Eq.1)}$$

Fluorescence measurements were performed at 30 °C by using TECAN Safire II using Magellan© software and Nunclon black flat-bottom 96-well plates. The excitation wavelength was set to 280 nm with a fluorescence intensity at 470 nm and the gain at 210. The equilibrium dissociation constants for ligands were determined by competitive binding with DNSA. A fixed

concentration of 20 μM DNSA and 0.25 μM hCA II Wt (180 μL) were then titrated against ligand from 0–32.5 μM (5~15 μL). The $K_d$ value ligands were then determined by fitting the data to equation 1 with Prism 9.0 software using the theorical $K_d$ of dansylamide for hCAII Wt ($K_{DNSA}$ = 9.6 nM) as described in the literature.[11] All the titration experiments were performed in triplicates.

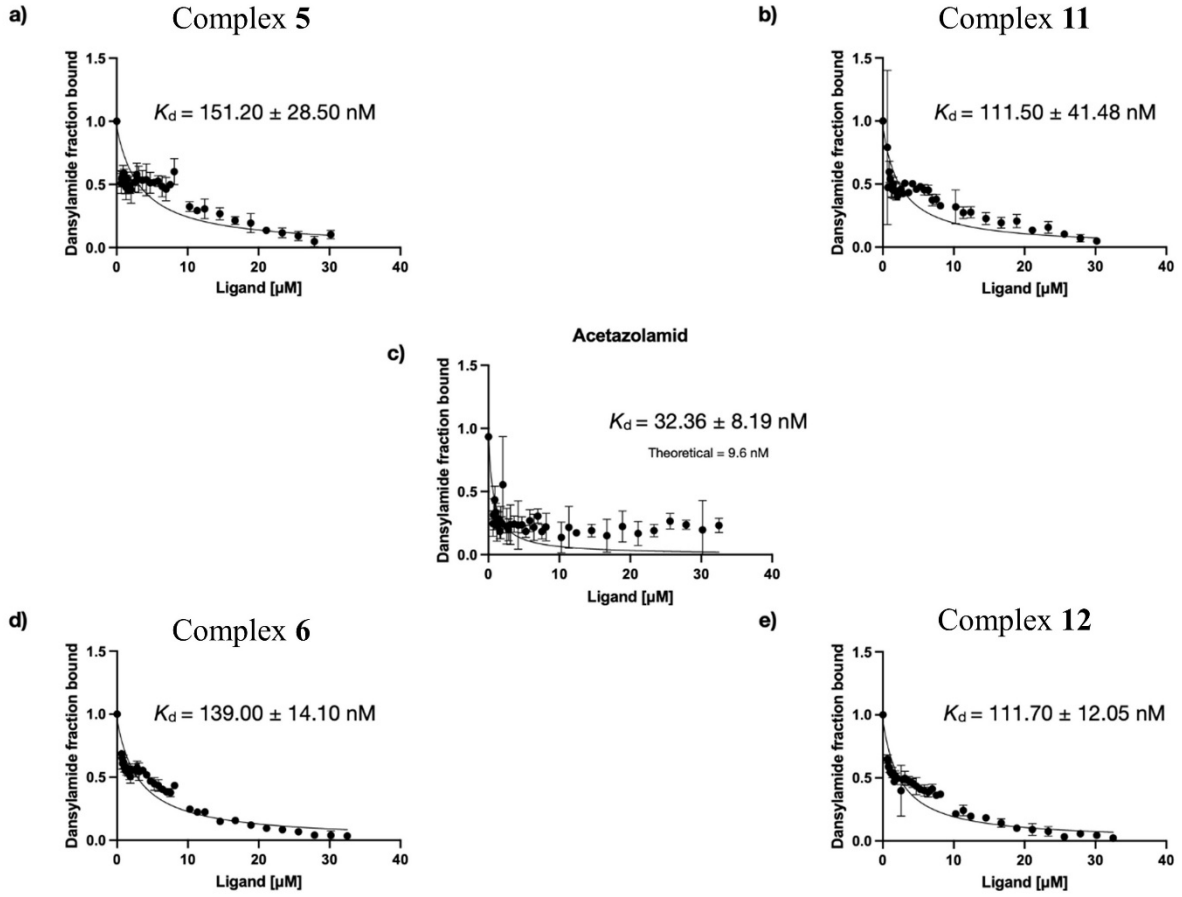


Determination of the dissociation constants for various ligand.

## 7. Cell culture

Human lung carcinoma (A549) cells were cultured using F12 media, Human breast (MD-MB-231) cells and retinal pigment epithelium (RPE1) cells using DMEM/F-12 medium supplemented with 10% FBS and 1% Penstrep. The cells were cultivated and maintained in a cell culture incubator at 37 °C with 5 % $CO_2$ and 20 % $O_2$ atmosphere for normoxia and 5 %

$CO_2$ and 2 % $O_2$ atmosphere for hypoxia. The hypoxia cells were passaged three times in hypoxia conditions and were cultured at least 15 days in hypoxia condition before the experiment.

## 8. Western Blotting

Prior to further analyses, endogenous CAIX expression at the protein level was confirmed by western blotting. The protein extract of cells from cancer cell lines (A549, MDA-MB-231) cultured in hypoxia and normoxia conditions, and a normal cell line (RPE-1) were sampled when the confluence reached 70%. Briefly, the attached cells were washed with ice-cold PBS three times and scraped to collect cell pellets. After removal of the PBS, a radio-immunoprecipitation assay (RIPA) lysis buffer containing protease inhibitors provided by the manufacturer (invitrogen, Thermo Fisher Scientific) was added into the cell pellets to obtain protein lysates. A Pierce$^{TM}$ BCA protein assay was conducted to measure the protein concentration of each cell lines and then protein (30 $\mu$g/lane/cell line) from each cell line was loaded onto a sodium dodecyl sulfate poly-acrylamide gel electrophoresis gel (SDS-PAGE) for separating the proteins into bands. The separated protein bands were transferred to nitrocellulose membranes (invitrogen, Thermo Fisher Scientific). The membranes were incubated with GAPDH antibodies (Abcam, Cambridge, UK; ab37168) at 1/100 or CAIX antibodies (Abcam, Cambridge, UK; ab184006) at a 1/1000 dilution overnight at 4°C. The resulting membranes were rinsed with Tris-buffered saline Tween-20 (TBS-T) three times for 5 minutes, and incubated with the Goat anti-rabbit lgG (H+L) (HRP)-conjugated secondary antibodies (invitrogen, Thermo Fisher Scientific) at 1/5000 for 2 h at room temperature. To detect immunereactive protein bands, enhanced chemiluminescence reagents (SuperSignalTM West Pico PLUS Chemiluminescent Substrate, Thermo Scientific) were used according to the manufacturer's instructions. The Western blots were quantified using ImageJ (1.53T).

## 9. CAIX confocal imaging

A549, MDA-MB-231 and RPE-1 cells ($1\times 10^5$ cells) were seeded in 35 mm dish with coverslip bottom (VWR, 734-2904) in normoxia (20% $O_2$) or hypoxia (2% $O_2$). All subsequent steps were performed at room temperature, except when otherwise stated. 48 h later, cells were fixed using 4% PFA in PBS for 15 min. After blocking (1h, 5% FBS in PBS), cells were incubated overnight at 4°C in primary CAIX antibody diluted 1/500 (Absolute Antibody, ref: 00414-1.1), then in Goat anti Mouse IgG (H+L) Alexa Fluor 647 secondary antibody 1/1000 (Invitrogen A-21235) for 2 h and finally in Hoechst 33342 nuclear stain (1 µg/mL) for 10 min. Cells were imaged in PBS in a confocal laser scanning microscope (Leica SP8, Leica Microsytemes SAS, Nanterre, France) equipped with an oil immersion x63/1.40 plan apochromat objective. The excitation/emission wavelengths were 405/420-450 nm (Hoechst) and 638/670-800 nm (Alexa Fluor 647). All acquisitions were performed with the same laser intensities and detection gains. To assess staining specificity, cells were stained as above but replacing the primary antibody by PBS.

## 10. Cellular uptake

A549 cells were seeded at a $4\times10^6$ cell density in 6 cm culture petridish at 37 °C, 5% $CO_2$, 20% $O_2$, After 24 h, the medium was replaced with 5 µM of complexes dilution in 10 mL of culture medium, and the dishes were incubated for 4 h at 37 °C, 5%$CO_2$. Cells were washed three times with cold PBS, trypsinized, and harvested, and a 10 µL aliquot of each cell suspension was sampled for accurate counting using a hemocytometer. The cell suspensions were centrifuged, and the supernatant was discarded. The pellets were digested in 100 µL of 70% $HNO_3$ at 65 °C for 16 h and then diluted in 5 mL of MilliQ water (final $HNO_3$ concentration: 1.4%). The Ru/Os content in each sample was determined by Inductively coupled plasma mass spectrometry (ICP-MS). The Ru/Os content was determined with an ICP-MS apparatus and the results compared with the Ru/Os references. The Ru/Os content was then associated with the number of cells.

## 11. Cellular fraction

A549 cells were seeded at a $4\times10^6$ cell density in 10 cm culture petridish at 37 °C, 5% $CO_2$. After 24 h, the medium was replaced with 5 μM of complexes dilution in 10 mL of culture medium, and the dishes were incubated for 24 h at 37 °C, 5% $CO_2$. Then cells were washed three times with cold PBS, trypsinized, and harvested, and a 10 μL aliquot of each cell suspension was sampled for accurate counting. The cell suspensions were centrifuged, and the supernatant was discarded. Then used NE-PER Nuclear and Cytoplasmic Extraction Reagents (Thermo fisher 78833) to isolate nuclei and cytoplasm. The pellets were obtained by freeze dryer and digested in 100 μL of 70% $HNO_3$ at 65 °C for 24 h, then diluted in 5 mL of MilliQ water (final $HNO_3$ concentration: 1.4%). The Ru/Os content in each sample was determined by Inductively coupled plasma mass spectrometry (ICP-MS). The Ru/Os content was determined with an ICP-MS apparatus and the results compared with the Ru/Os references. The Ru/Os content was then associated with the number of cells.

## 12.Cellular uptake inhibition mechanism studies

A549 cells were preincubated with carbonic anhydrase inhibitor (acetazolamide, 50 μM) for 2 h. After this time, the cells were washed by PBS for 3 times and then incubated with the sample (5 μM) for 4 h at 37 °C and then washed with PBS. The cells were detached with trypsin, harvested, centrifuged, and resuspended. The number of cells on the dish was counted. The sample was digested using a 70% $HNO_3$ solution at 65 °C for 24 h and then diluted in 5 mL of MilliQ water (final $HNO_3$ concentration: 1.4 %). The Ru/Os content was determined with an ICP-MS apparatus and the results compared with the Ru/Os references. The Ru/Os content was then associated with the number of cells.

## 13.Ru complexes confocal imaging

A549 cells (1× $10^5$ cells) were seeded in 35 mm culture dishes as detailed above. 24 h later, culture medium was replaced by fresh medium containing 5 μM of complex **3** or 5 μM of complex **6**, respectively. After incubation for 4 h in the dark at 37°C, cells were washed with PBS. Cells were then stained with Hoechst 33342 (1 μg/mL) and Green CellMask (100 nM, Invitrogen), MitoTracker Green (MTG, 100 nM, Invitrogen) at room temperature for 10 min, and LysoTracker Green (LTG, 100 nM, Invitrogen) for 40min. Live cells were imaged in a confocal laser scanning microscope (Leica SP8) equipped with an oil immersion x63/1.40 plan apochromat objective. The excitation/emission wavelengths were 405/420-450 nm (Hoechst), 488/670-800 nm (**Complex 3 and Complex 6),** 488/500-550 nm for Green CellMask, MTG and LTG, respectively. Care was taken to keep laser intensities as low as possible to avoid any phototoxicity.

## 14.(Photo-)toxicity

The phototoxicity of the complexes were assessed by measuring the cell viability using a fluorometric resazurin assay.[12] The cultivated cells were seeded in sextuplicate in 96 well plates with a density of 4000 cells per well in 100 μL of media. After 24 h, the medium was removed and the cells were treated with increasing concentrations of the complex diluted in cell media achieving a total volume of 100 μL at 37 °C with 5% $CO_2$ and 20 % $O_2$ atmosphere in normoxia condition for 4 h or 5% $CO_2$ and 2 % $O_2$ atmosphere in hypoxia condition for 4 h. Then the media was replaced with 100 μL fresh medium, plates were irradiated at different light wavelength (540 nm for 40 min (light dose 9.0 J/$cm^2$), 620 nm for 60 min (light dose 6.7 J/$cm^2$), 670 nm for 60 min (light dose 13.5 J/$cm^2$) and 740 nm for 60 min (light dose 12.6 J/$cm^2$) at 37 °C using a LUMOS-BIO photoreactor (Atlas Photonics) in normoxia and hypoxia, respectively. Then cells were cultivated for another 44 h, the media was changed with fresh media containing resazurin with a final concentration of 0.2 mg/mL. After 4 h of incubation at 37 °C, the fluorescence signal of resorufin product was measured ($\lambda_{ex}$: 540 nm and $\lambda_{em}$: 590

nm) in a BioTek®. $IC_{50}$ values were then calculated using GraphPad Prism software. Each experiment was performed in duplicate and an average $IC_{50}$ value (in μM) was reported with a standard deviation.

## 15.Figures

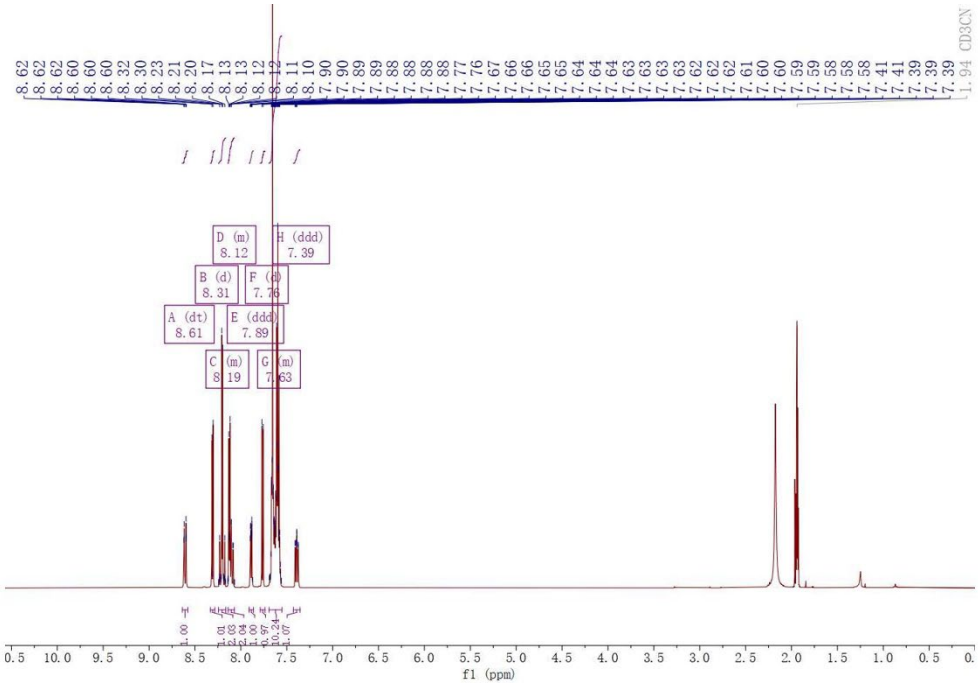


**Figure S 1.** $^{1}$H-NMR spectrum of **1** in $CD_3CN$, 400 MHz

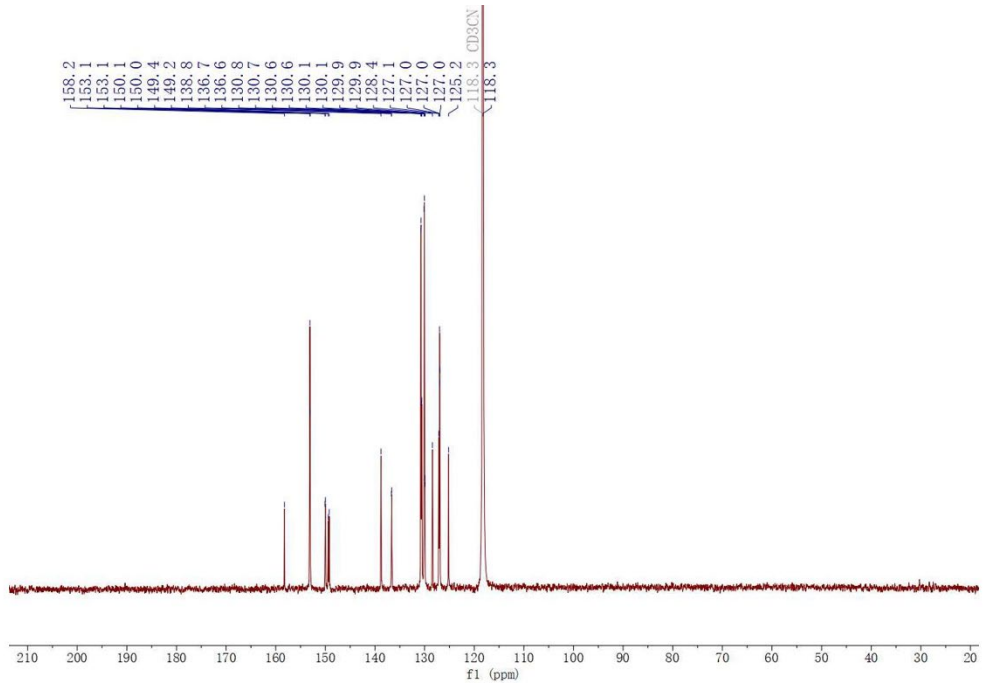


**Figure S 2.** $^{13}$C-NMR spectrum of **1** in $CD_3CN$, 101 MHz.

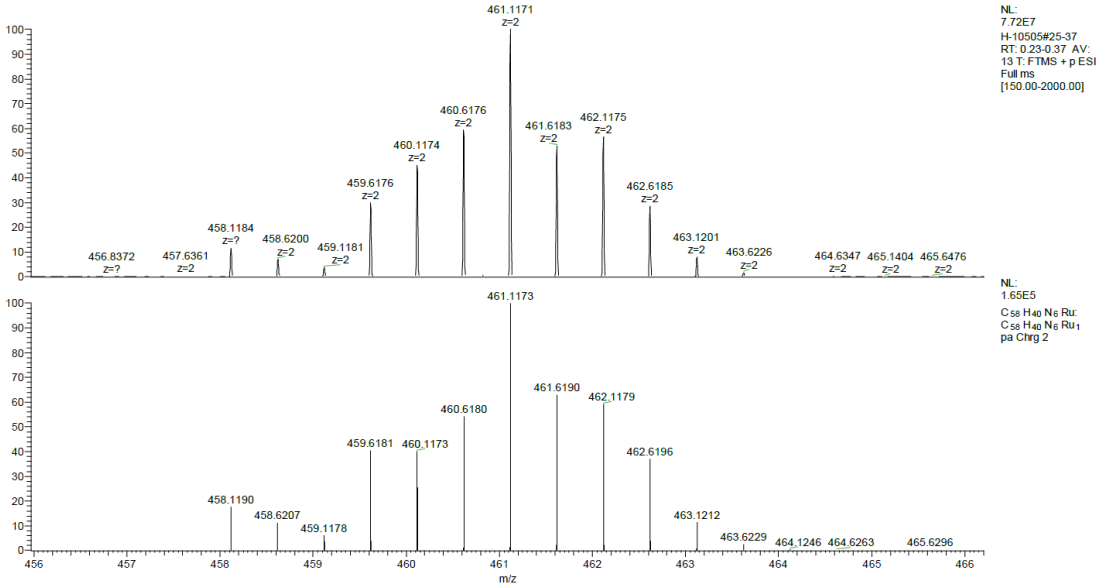


**Figure S 3.** (Experimental/Theoretical) ESI-HRMS spectrum of **1** (positive detection mode).

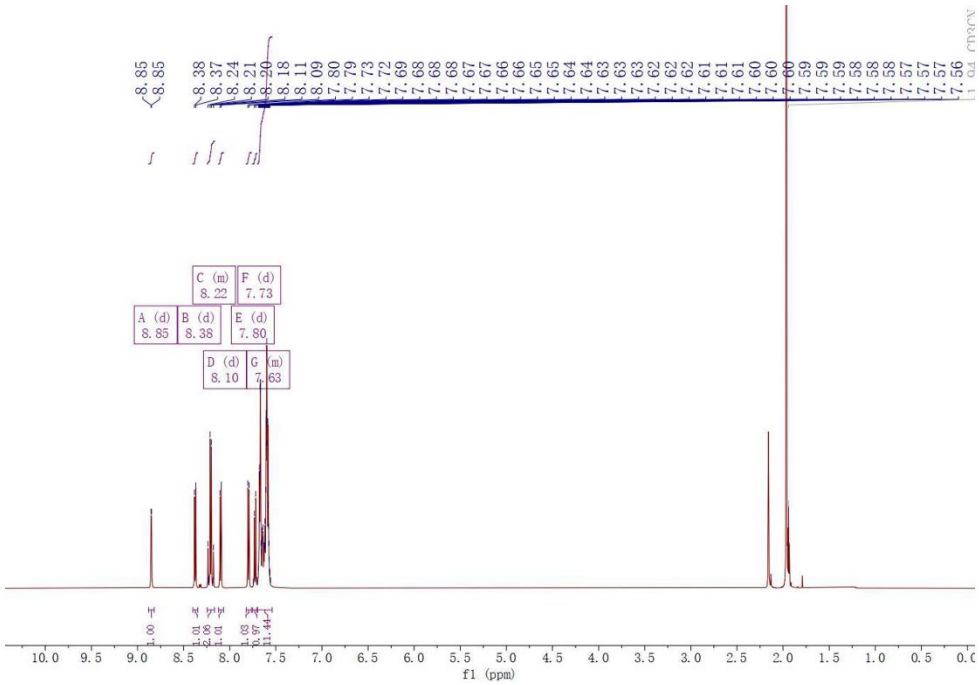


**Figure S 4.** $^{1}$H-NMR spectrum of **2** in $CD_3CN$, 400 MHz

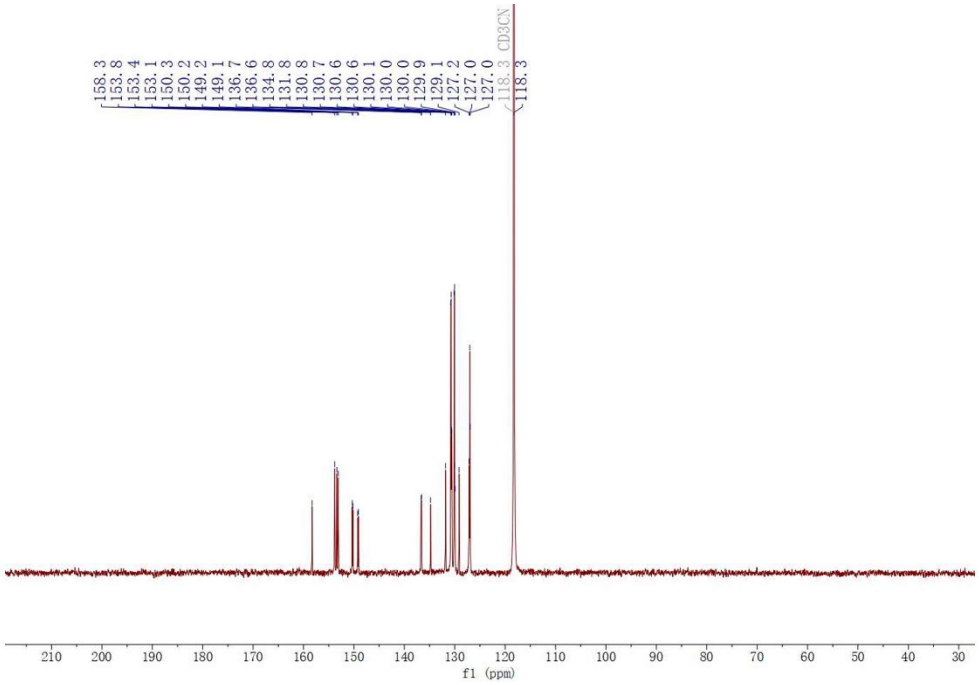


**Figure S 5.** $^{13}$C-NMR spectrum of **2** in $CD_3CN$, 101 MHz.

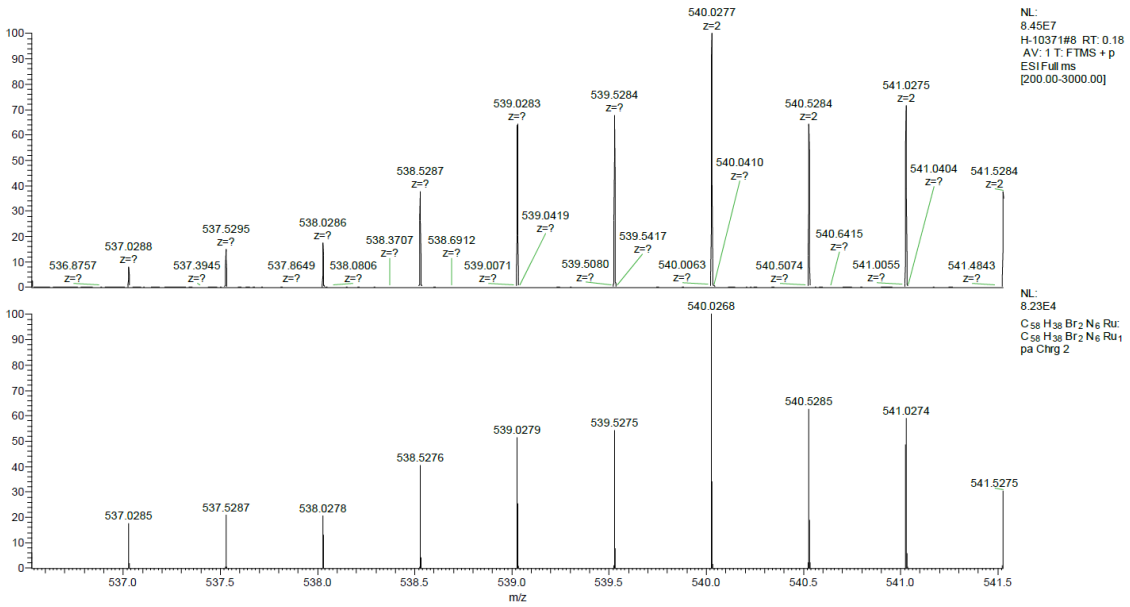


**Figure S 6.** (Experimental/Theoretical) ESI-HRMS spectrum of **2** (positive detection mode).

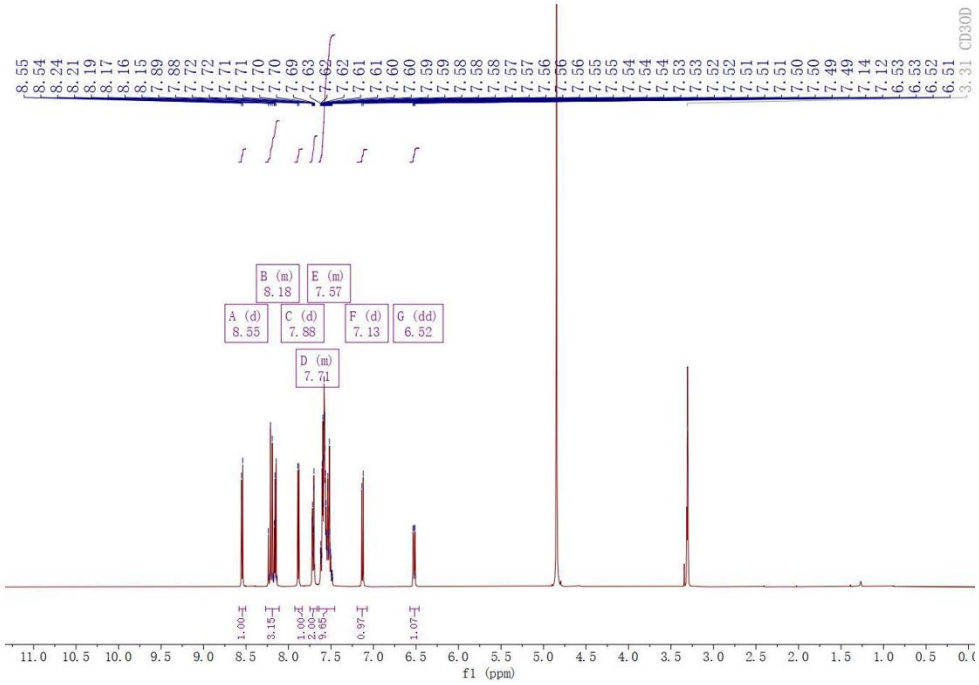


**Figure S 7.** $^{1}$H-NMR spectrum of **3** in $CD_3OD$, 400 MHz

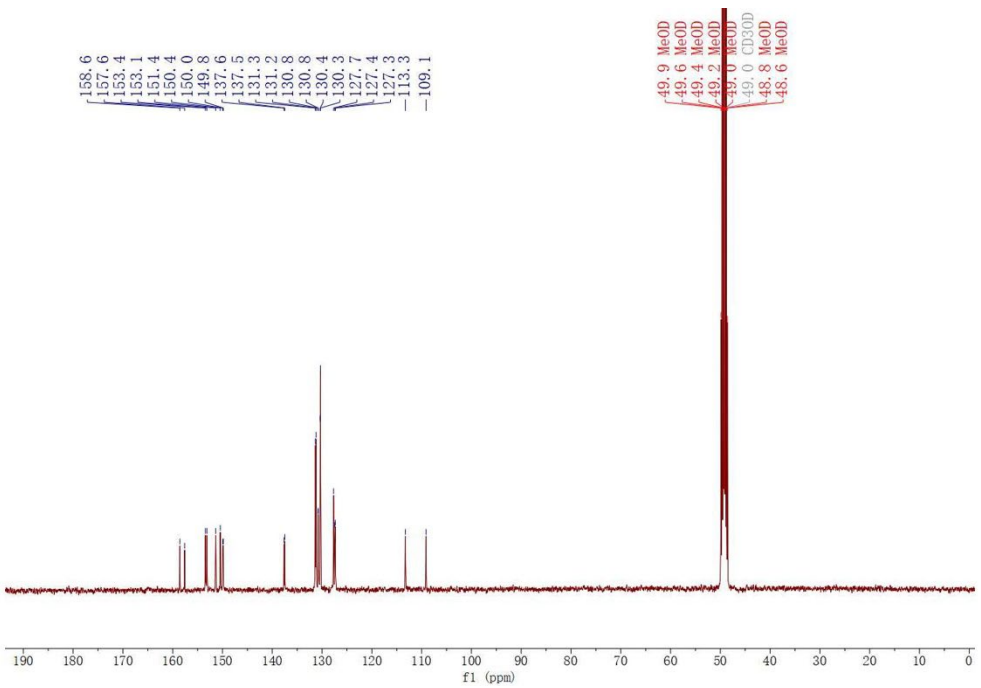


**Figure S 8.** $^{13}$C-NMR spectrum of **3** in $CD_3OD$, 101 MHz.

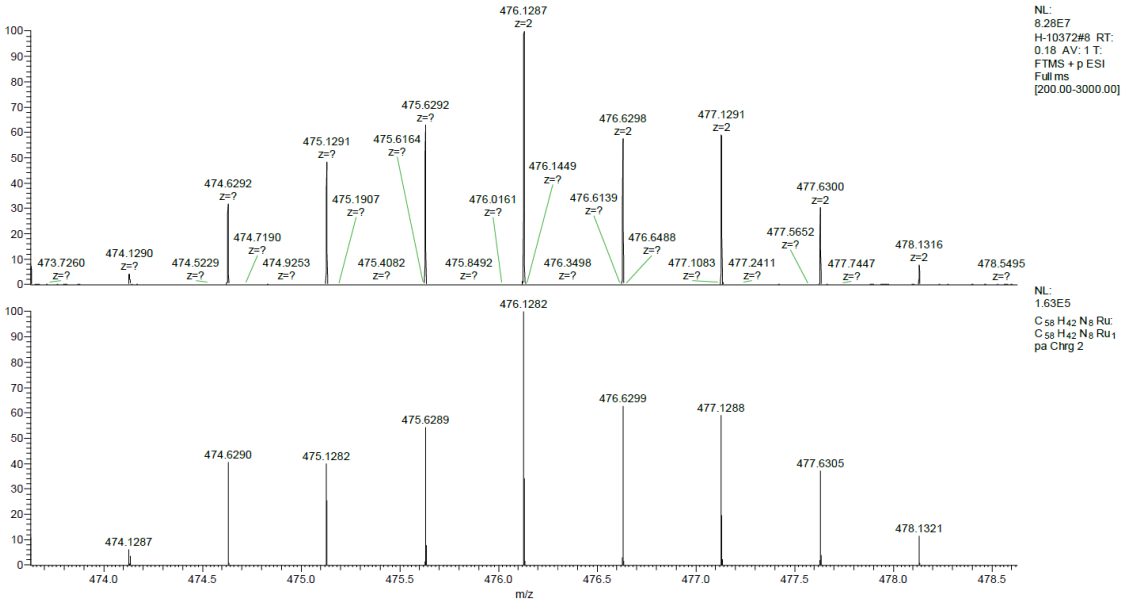


**Figure S 9.** (Experimental/Theoretical) ESI-HRMS spectrum of **3** (positive detection mode).

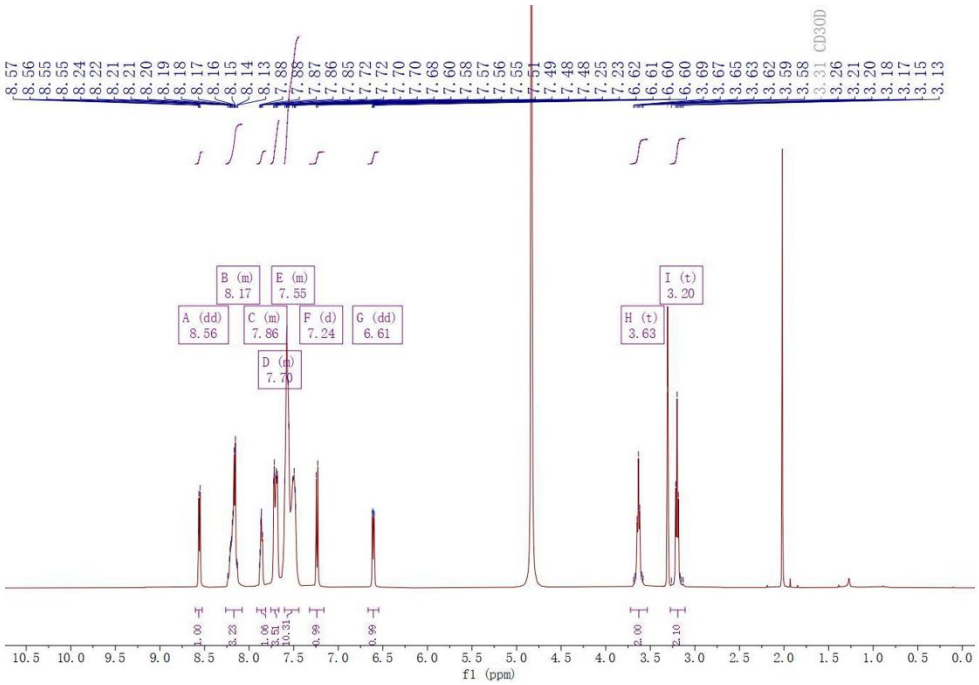


**Figure S 10.** [1]H-NMR spectrum of **4** in MeOD, 400 MHz

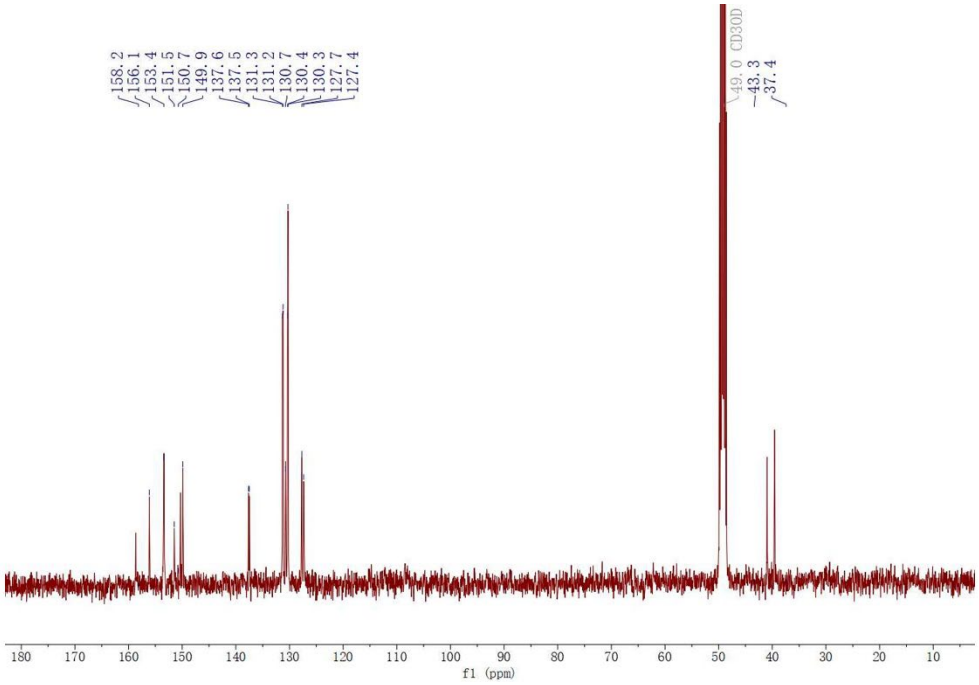


**Figure S 11.** [13]C-NMR spectrum of **4** in MeOD, 101 MHz.

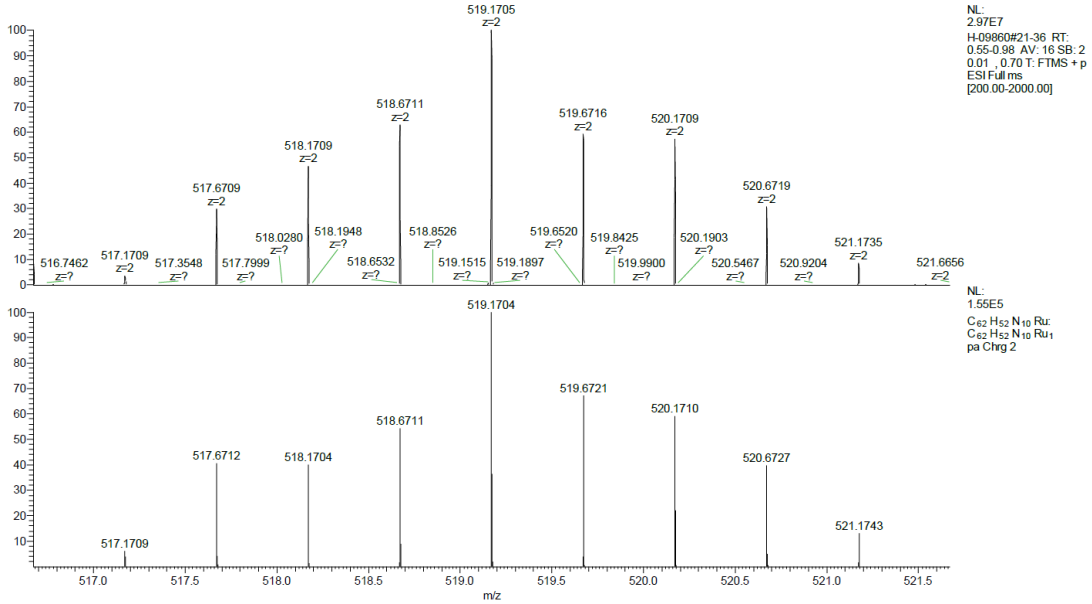


**Figure S 12.** (Experimental/Theoretical) ESI-HRMS spectrum of **4** (positive detection mode).

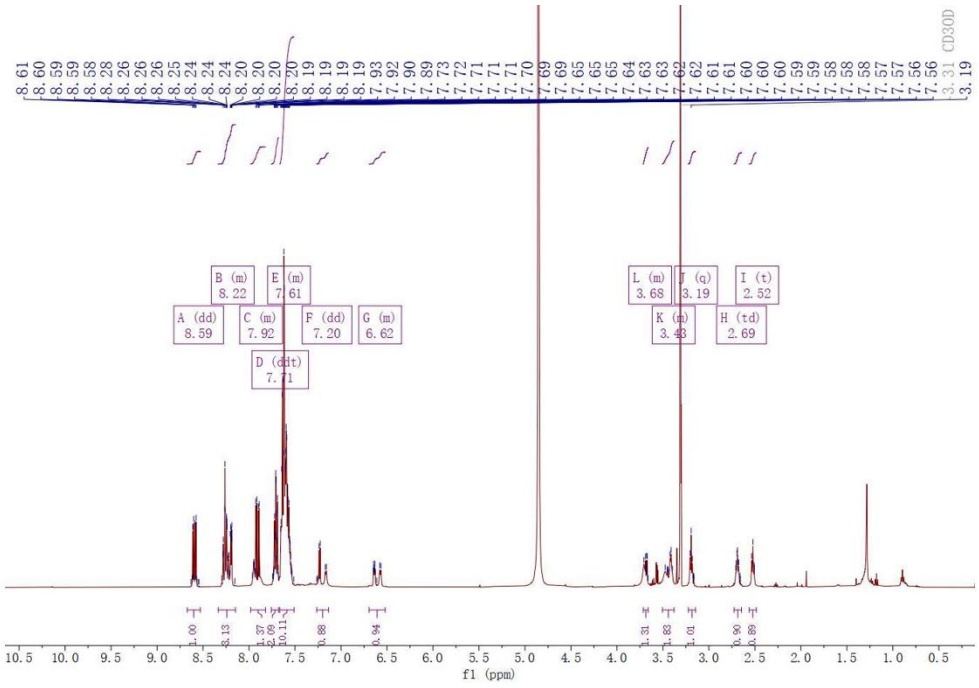


**Figure S 13.** $^{1}$H-NMR spectrum of **5** in $CD_3CN$, 400 MHz

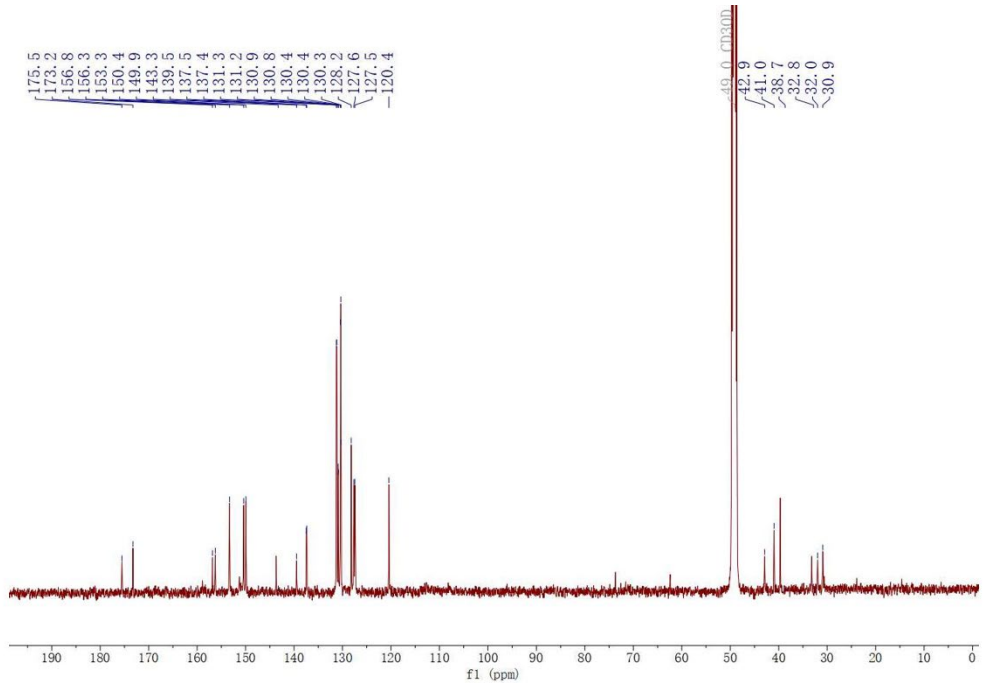


**Figure S 14.** $^{13}$C-NMR spectrum of **5** in $CD_3CN$, 126 MHz.

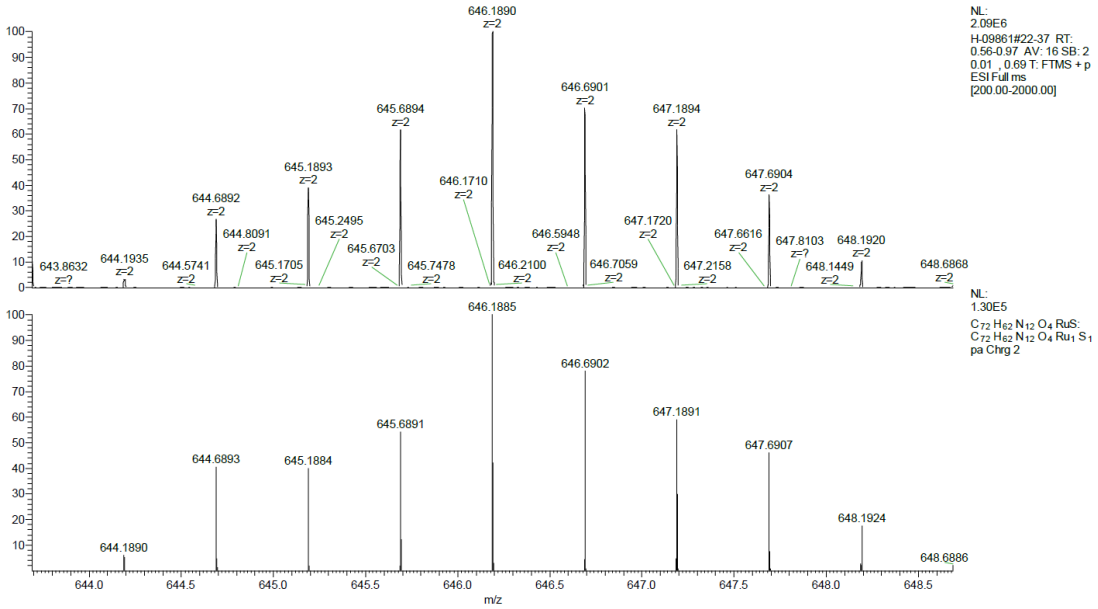


**Figure S 15.** (Experimental/Theoretical) ESI-HRMS spectrum of **5** (positive detection mode).

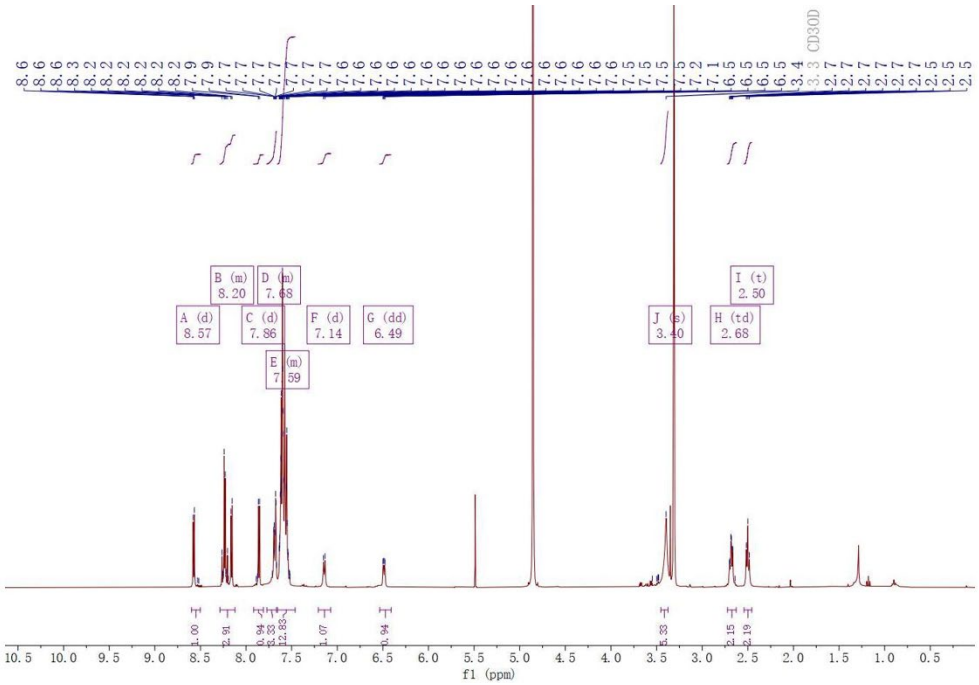


**Figure S 16.** $^{1}$H-NMR spectrum of **6** in MeOD, 400 MHz

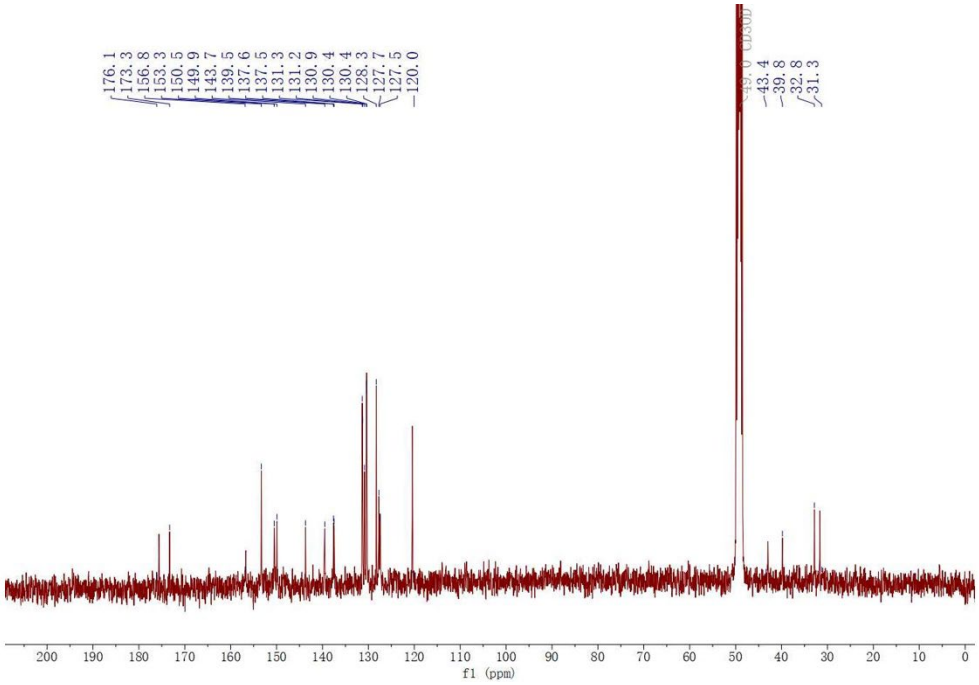


**Figure S 17.** $^{13}$C-NMR spectrum of **6** in $CD_3CN$, 101 MHz.

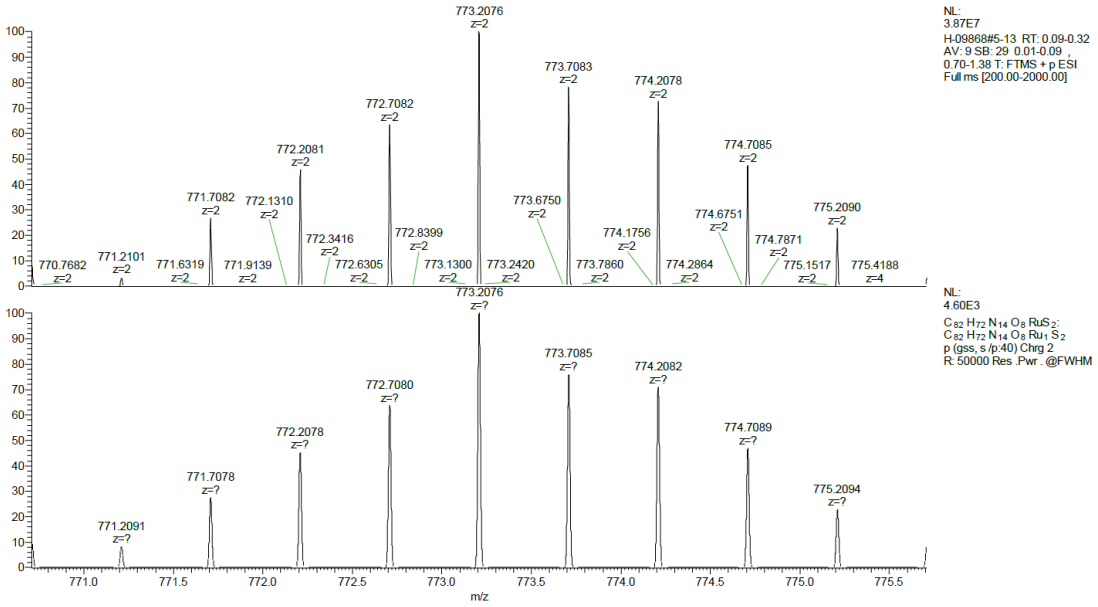


**Figure S 18.** (Experimental/Theoretical) ESI-HRMS spectrum of **6** (positive detection mode).

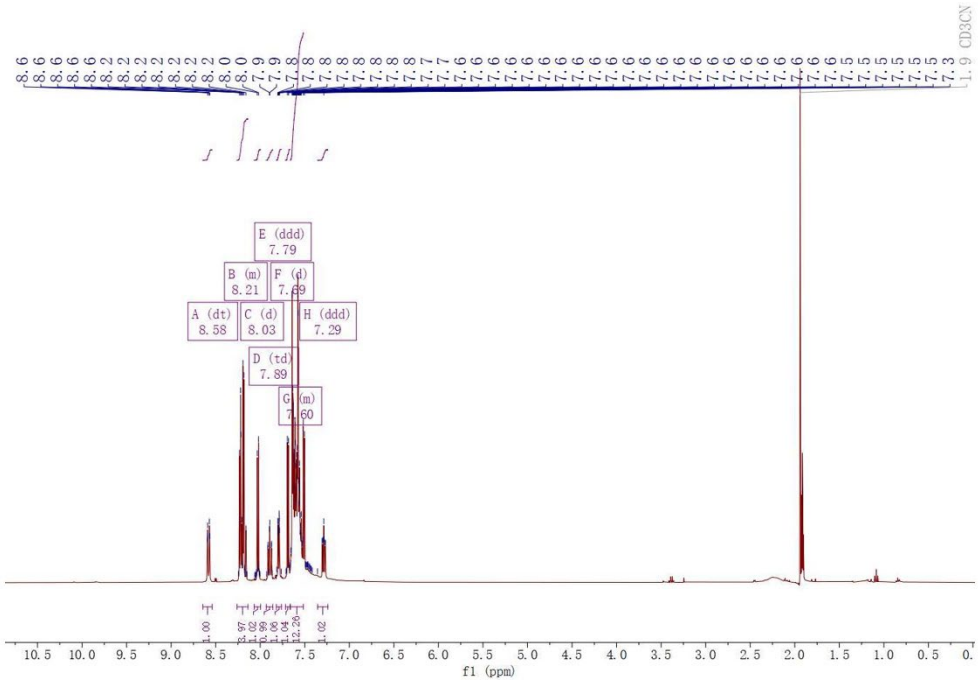


**Figure S 19.** $^{1}$H-NMR spectrum of **7** in $CD_3CN$, 400 MHz

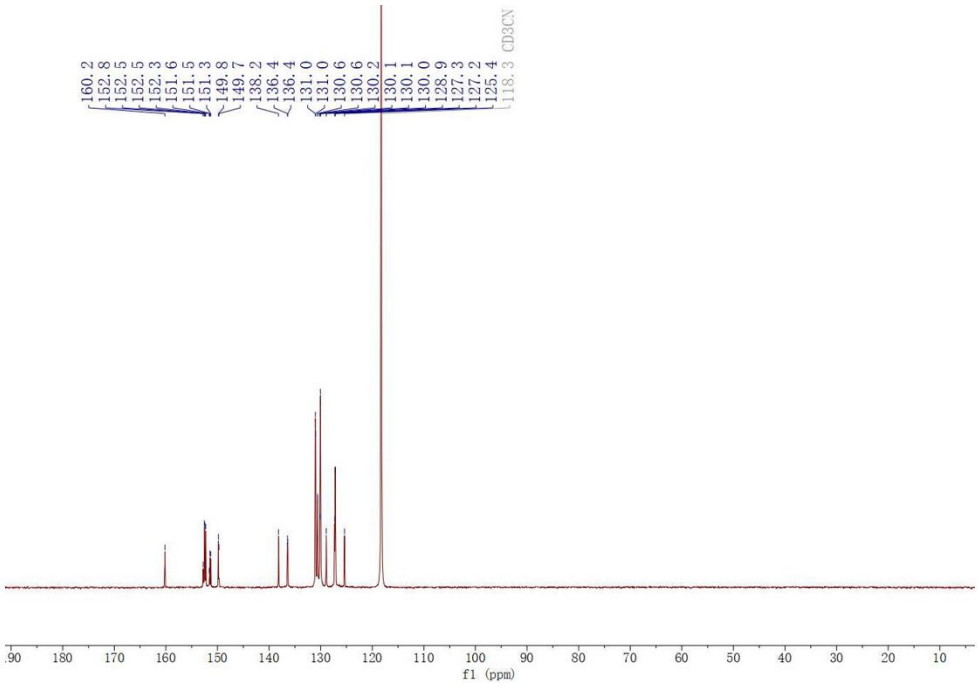


**Figure S 20.** $^{13}$C-NMR spectrum of **7** in $CD_3CN$, 101 MHz.

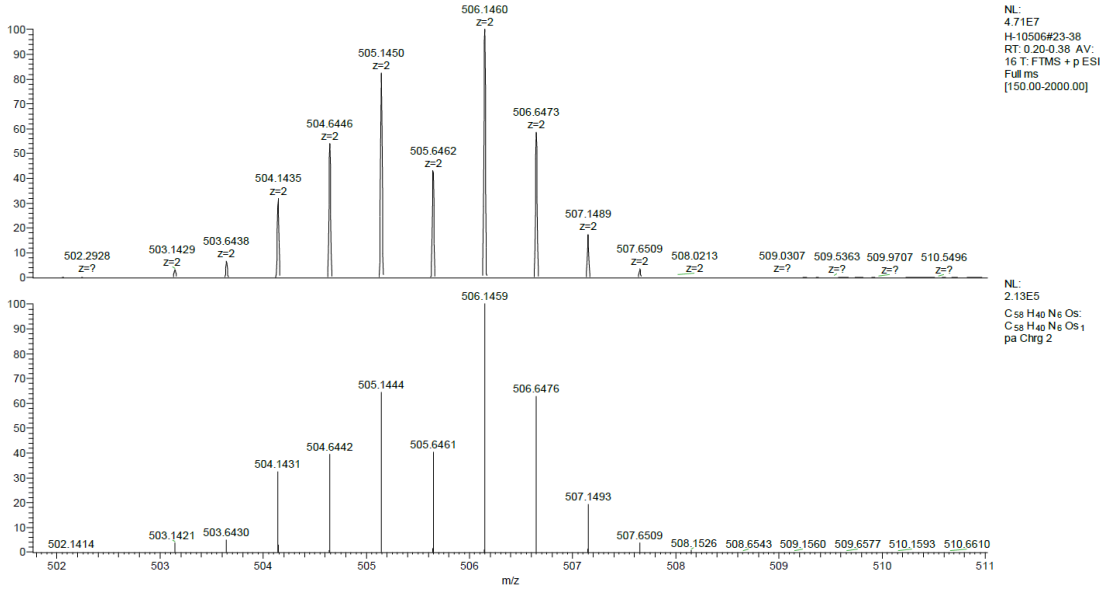


**Figure S 21.** (Experimental/Theoretical) ESI-HRMS spectrum of **7** (positive detection mode).

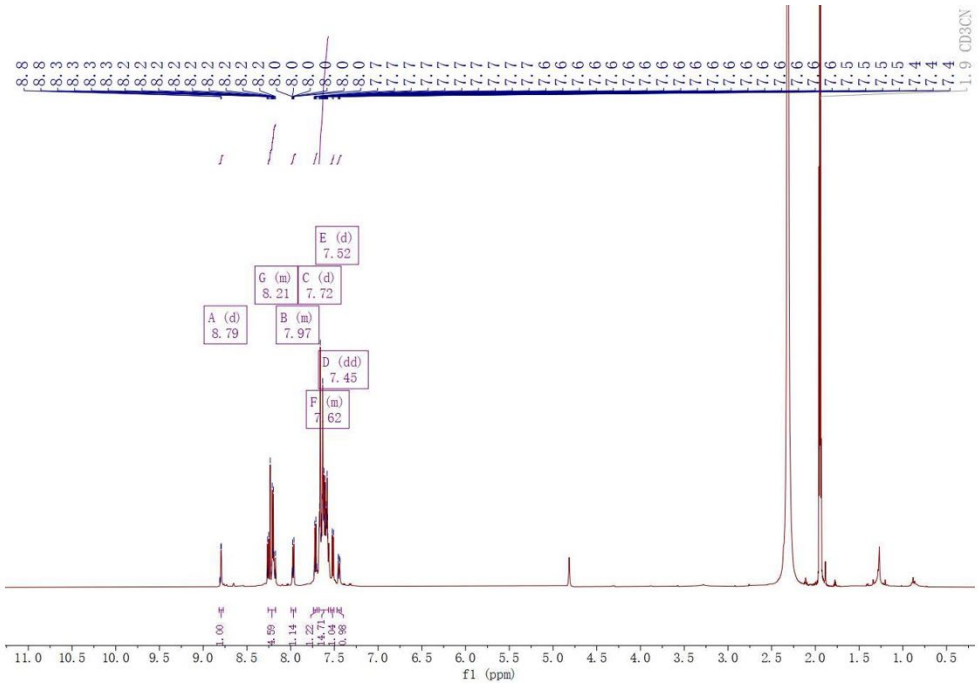


**Figure S 22.** $^{1}$H-NMR spectrum of **8** in $CD_3CN$, 400 MHz

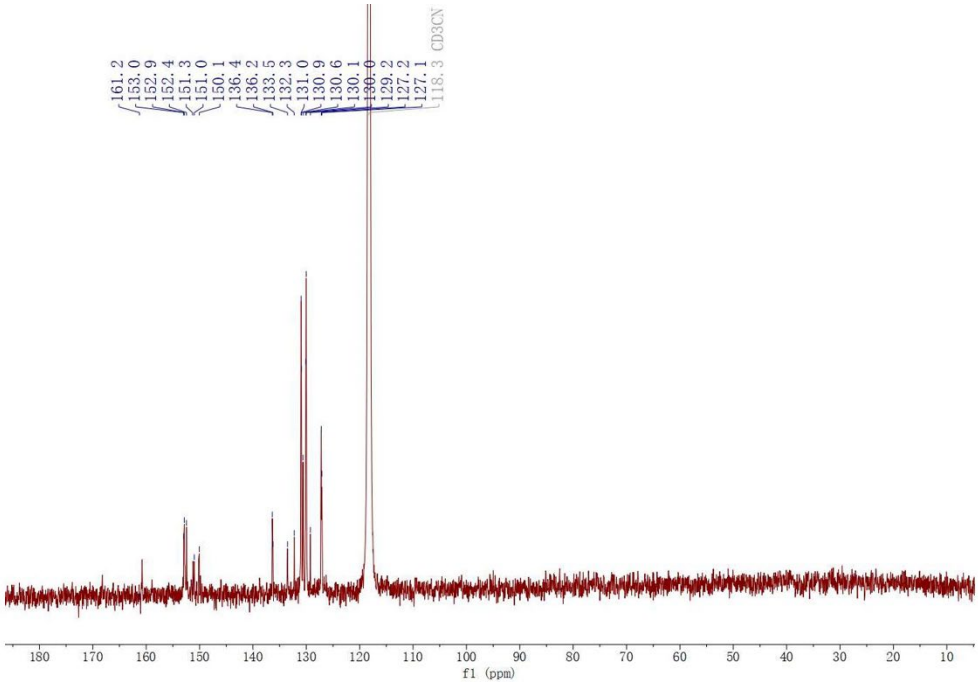


**Figure S 23.** $^{13}$C-NMR spectrum of **8** in $CD_3CN$, 101 MHz.

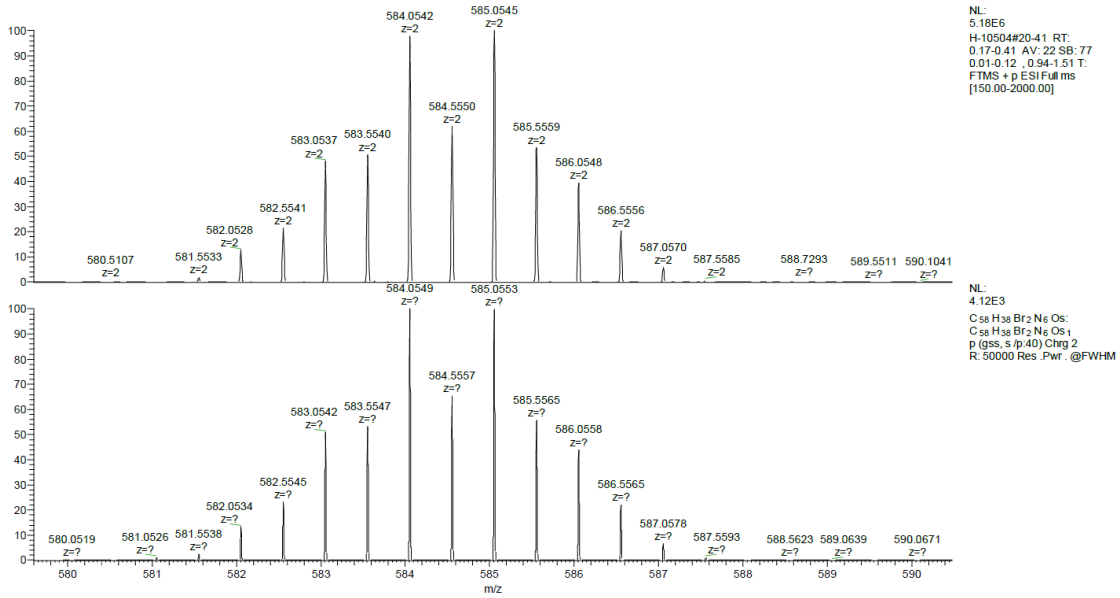


**Figure S 24.** (Experimental/Theoretical) ESI-HRMS spectrum of **8** (positive detection mode).

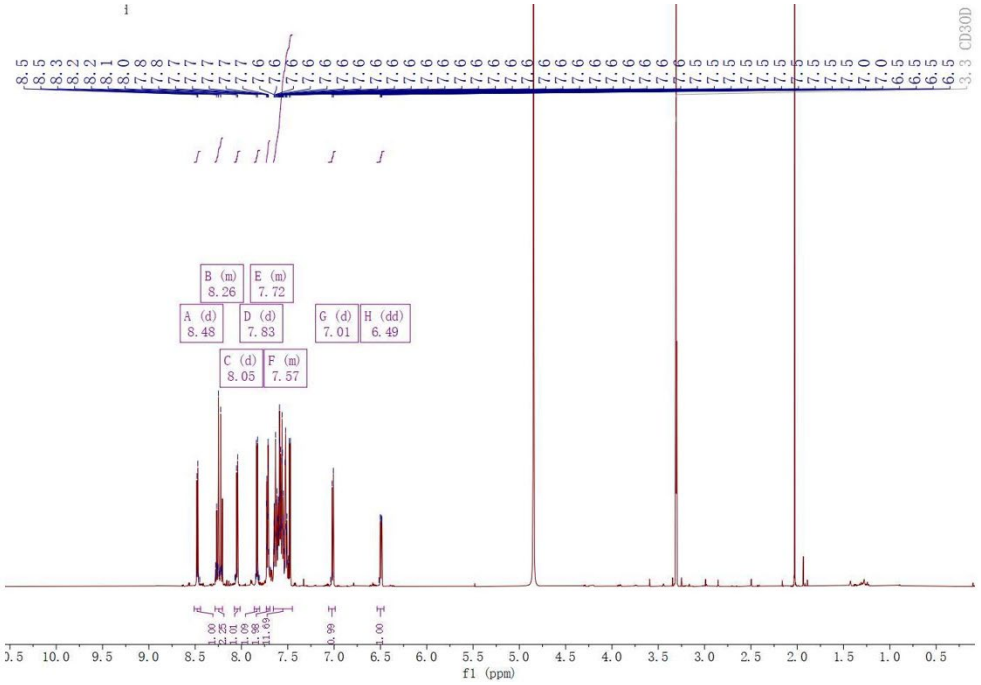


**Figure S 25.** $^{1}$H-NMR spectrum of **9** in MeOD, 500 MHz

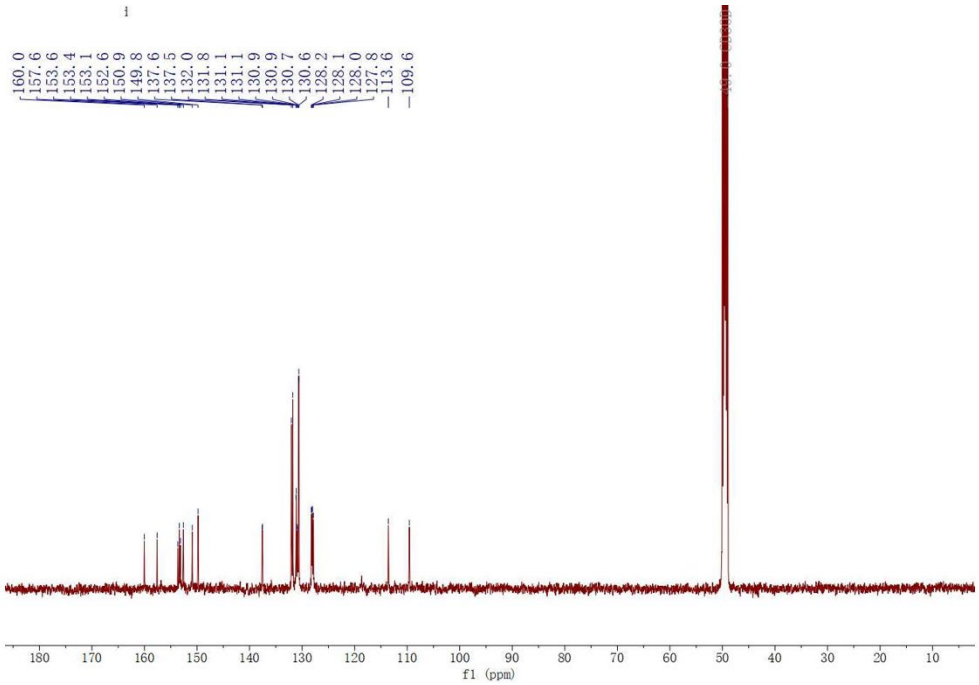


**Figure S 26.** $^{13}$C-NMR spectrum of **9** in MeOD, 126 MHz.

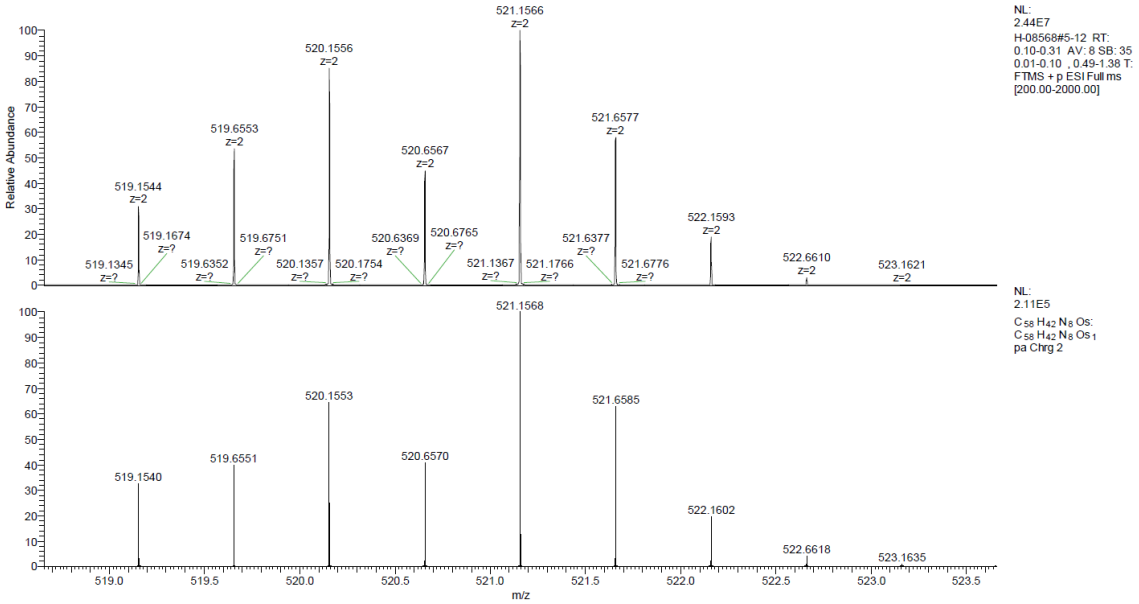


**Figure S 27.** (Experimental/Theoretical) ESI-HRMS spectrum of **9** (positive detection mode).

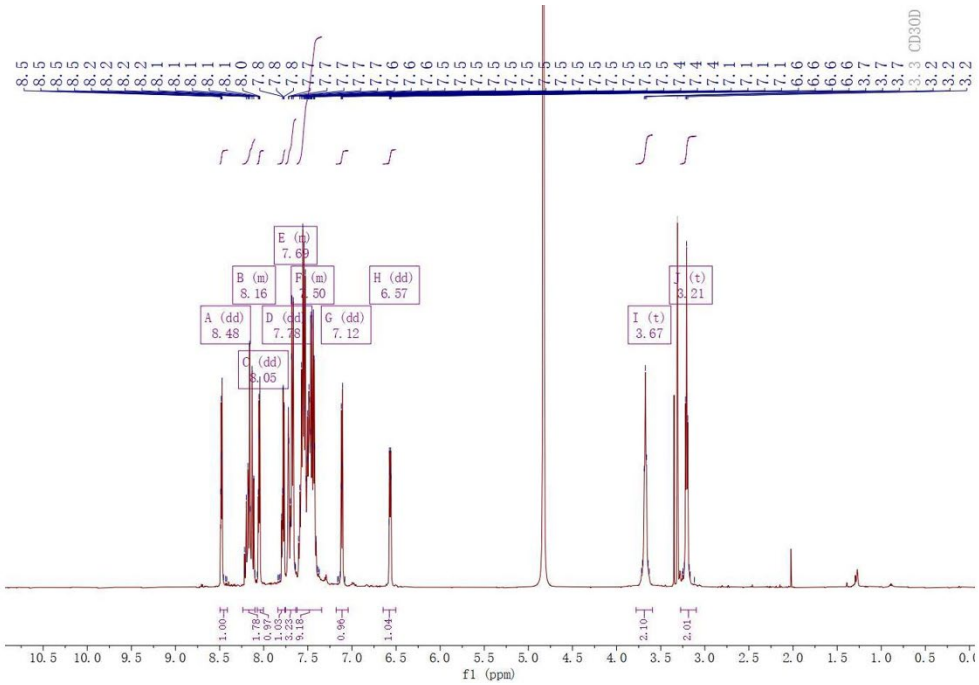


**Figure S 28.** [1]H-NMR spectrum of **10** in MeOD, 500 MHz

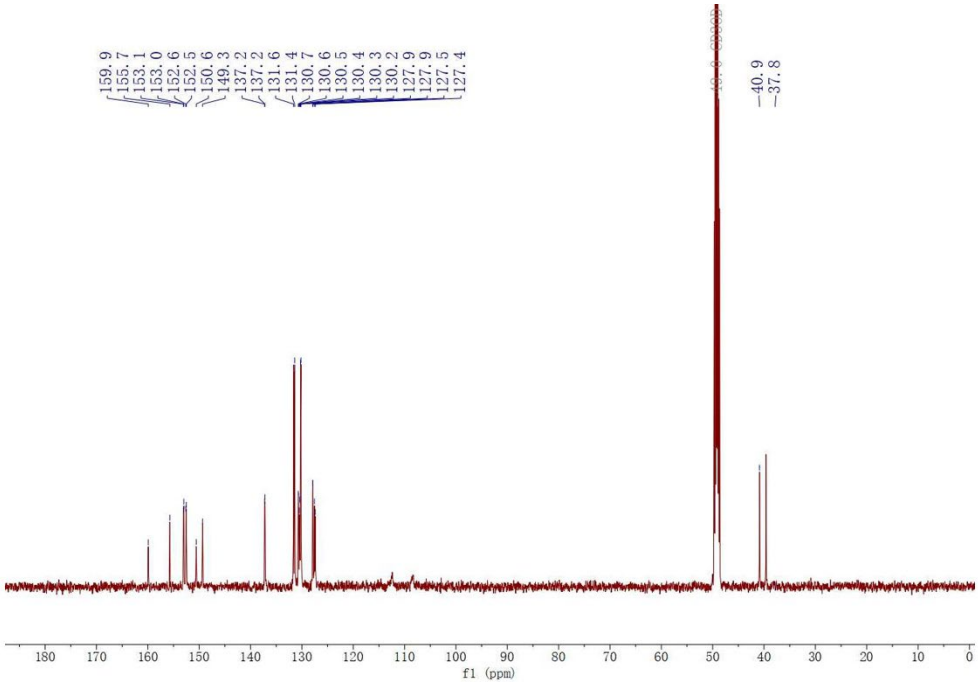


**Figure S 29.** [13]C-NMR spectrum of **10** in MeOD, 126 MHz.

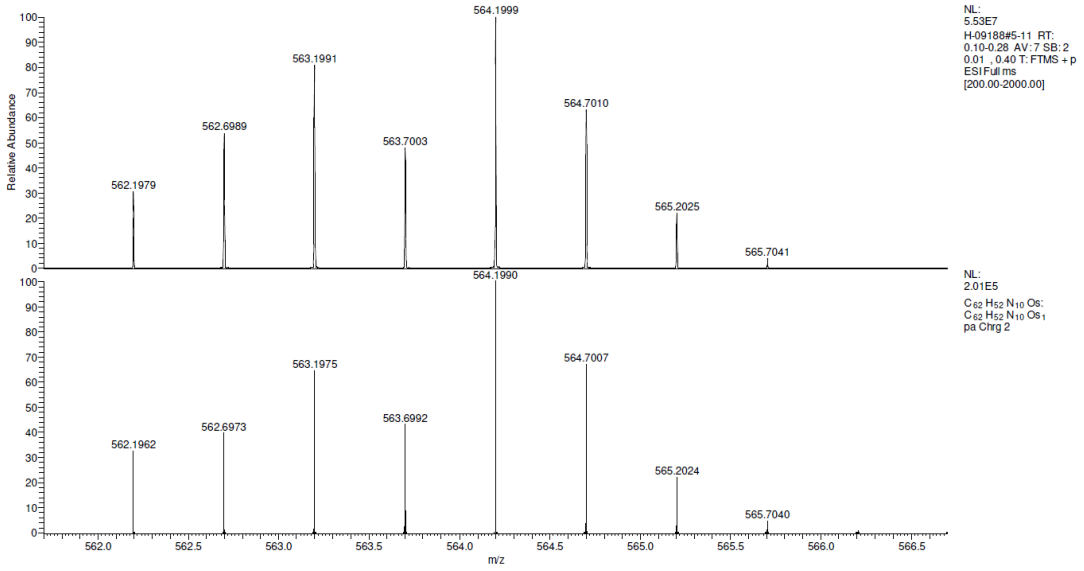


**Figure S 30.** (Experimental/Theoretical) ESI-HRMS spectrum of **10** (positive detection mode).

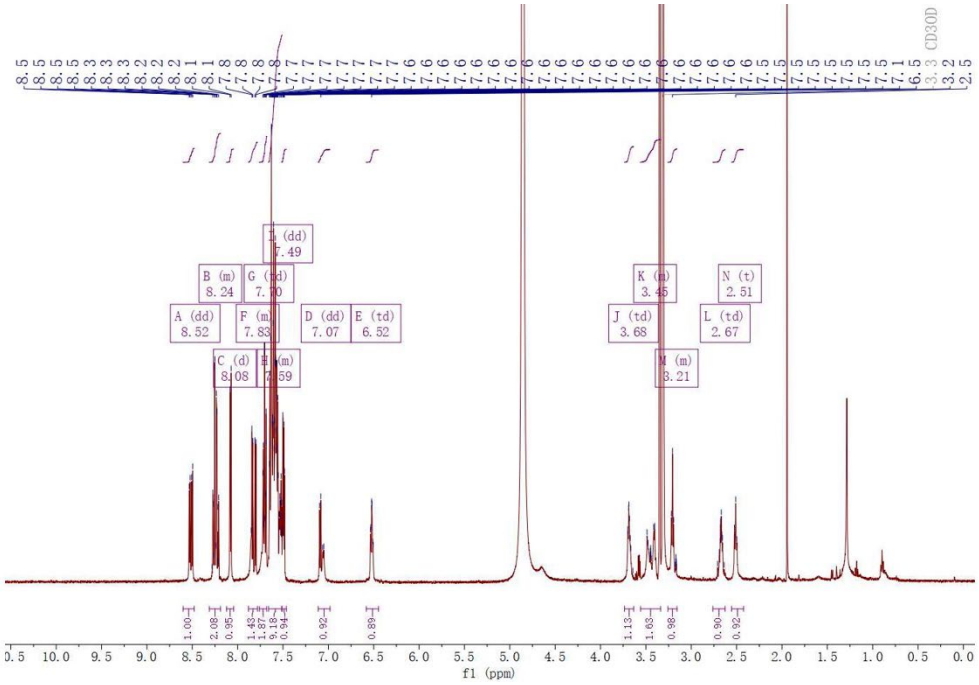


**Figure S 31.** $^{1}$H-NMR spectrum of **11** in MeOD, 500 MHz

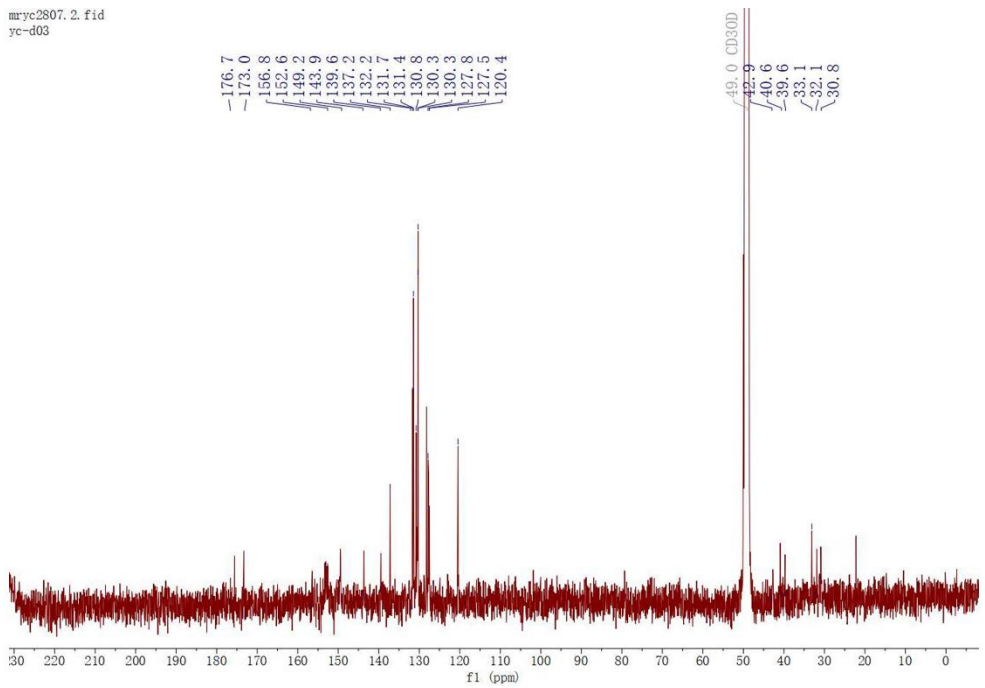


**Figure S 32.** $^{13}$C-NMR spectrum of **11** in MeOD, 126 MHz.

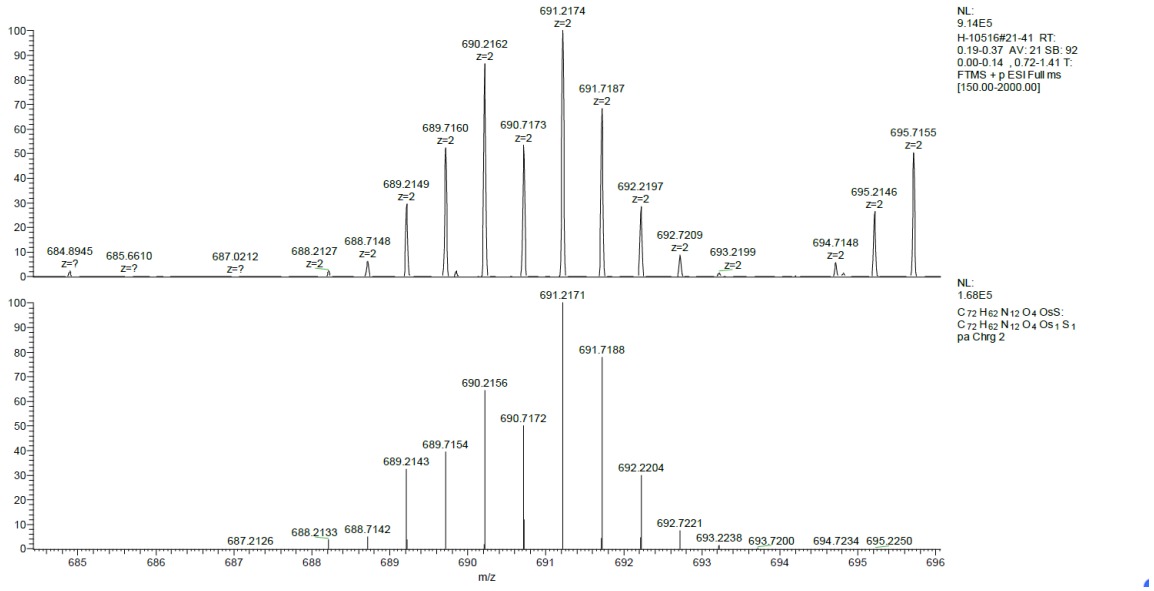


**Figure S 33.** (Experimental/Theoretical) ESI-HRMS spectrum of **11** (positive detection mode).

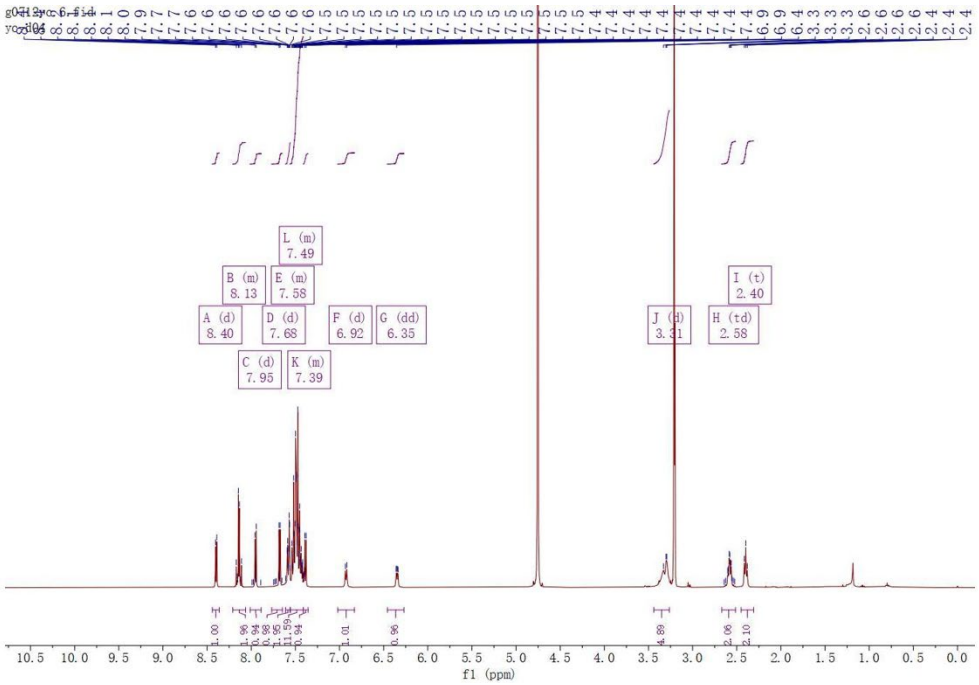


**Figure S 34.** [1]H-NMR spectrum of **12** in MeOD, 400 MHz

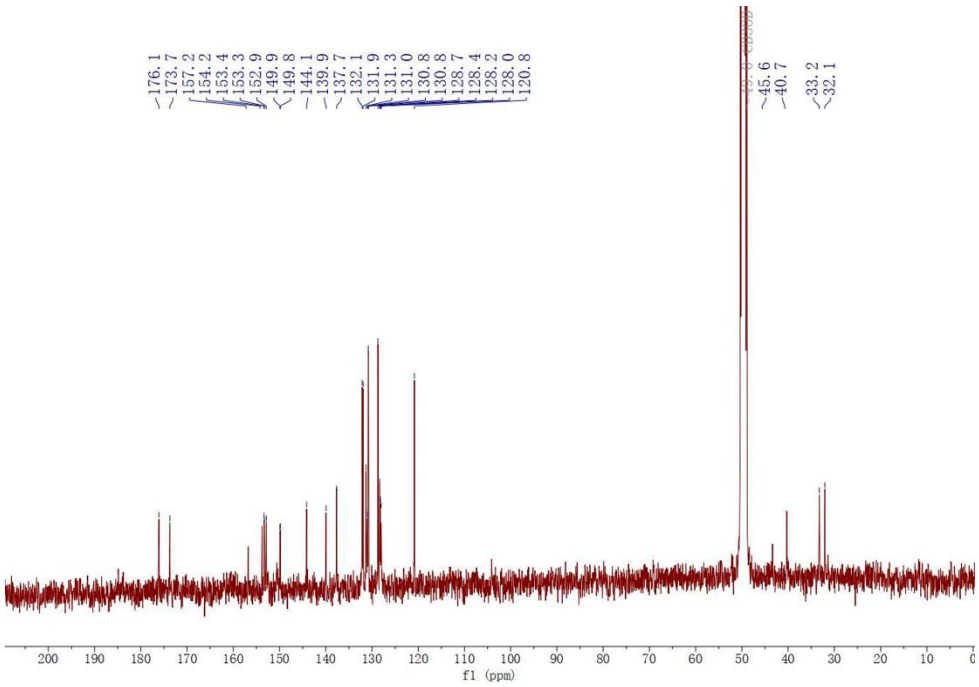


**Figure S 35.** [13]C-NMR spectrum of **12** in MeOD, 101 MHz.

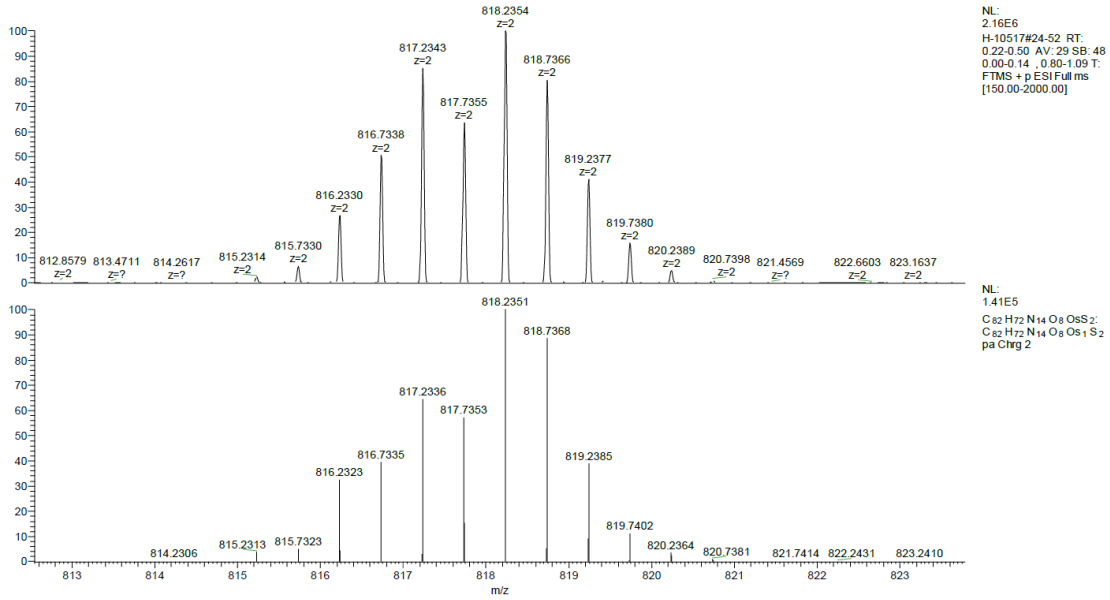


**Figure S 36.** (Experimental/Theoretical) ESI-HRMS spectrum of **12** (positive detection mode).

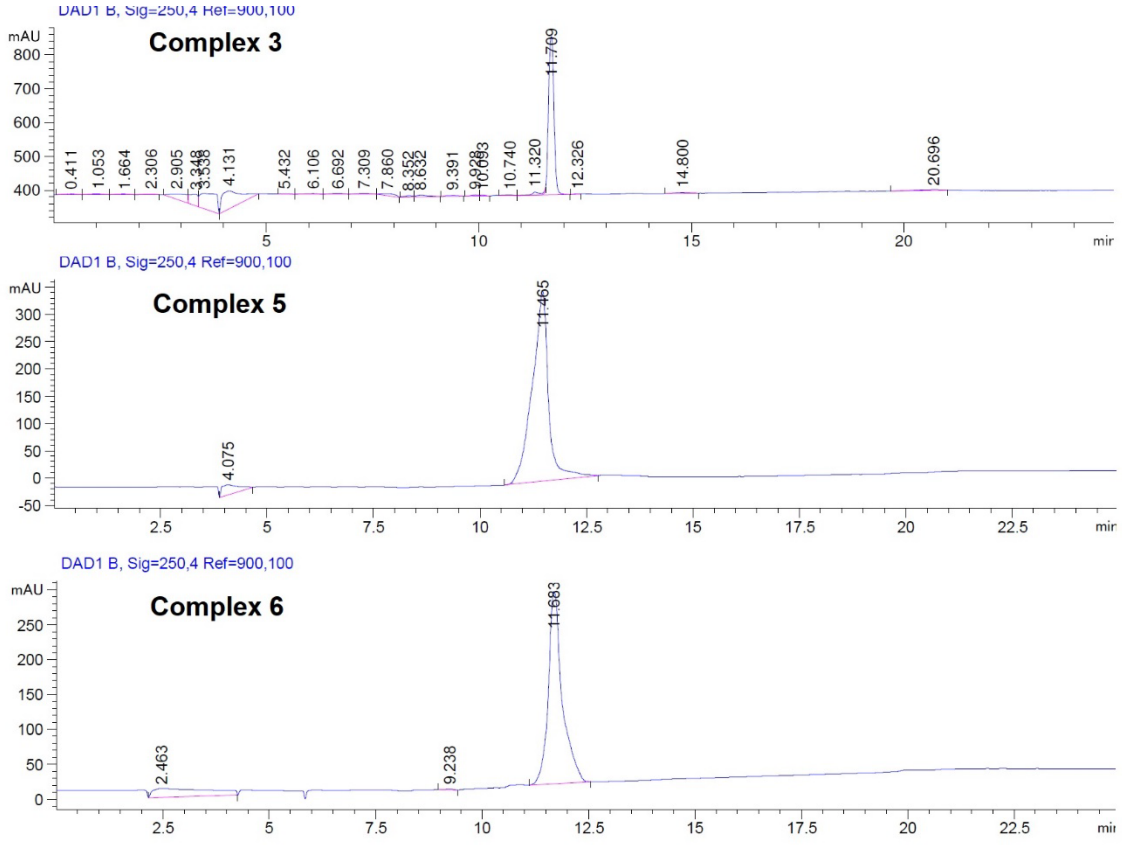


**Figure S 37.** Analytic HPLC of the Ru-based complexes **3**, **5** and **6** with detection at 250 nm.

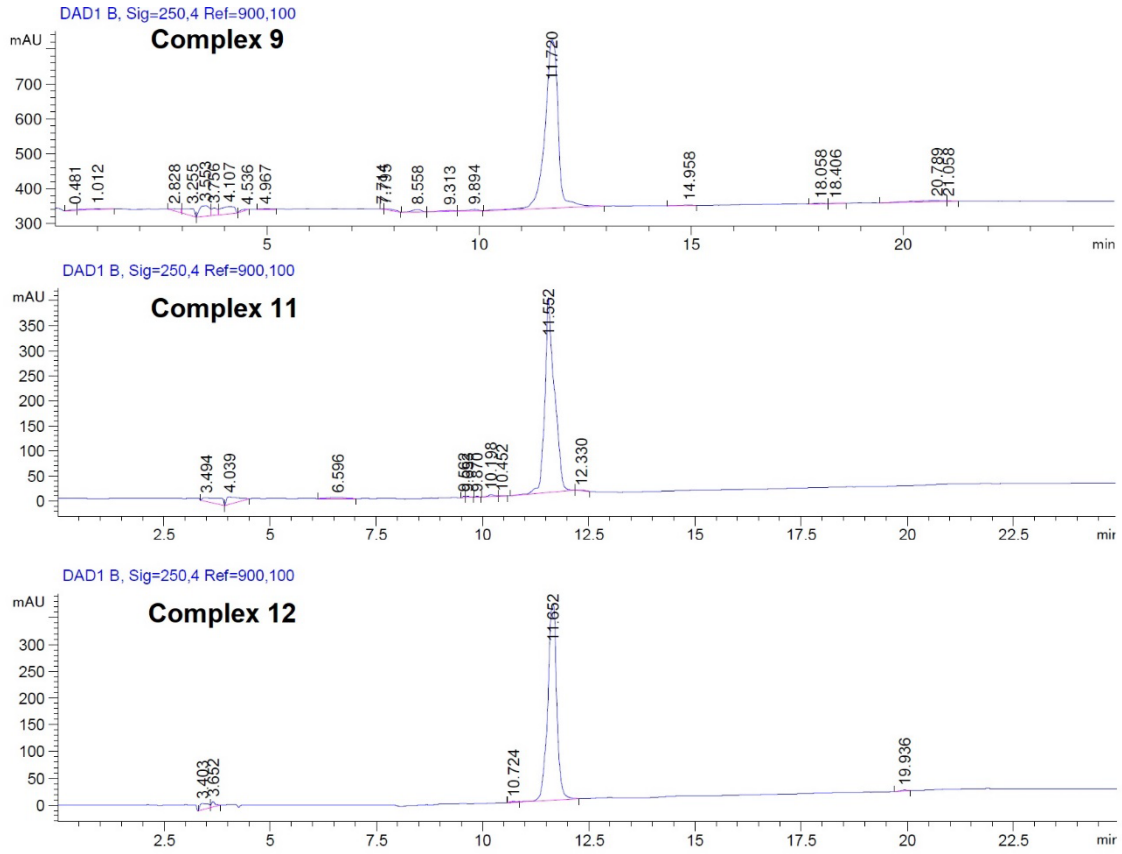


**Figure S 38.** Analytic HPLC of the Ru-based complexes 9, 11 and 12 with detection at 250 nm.

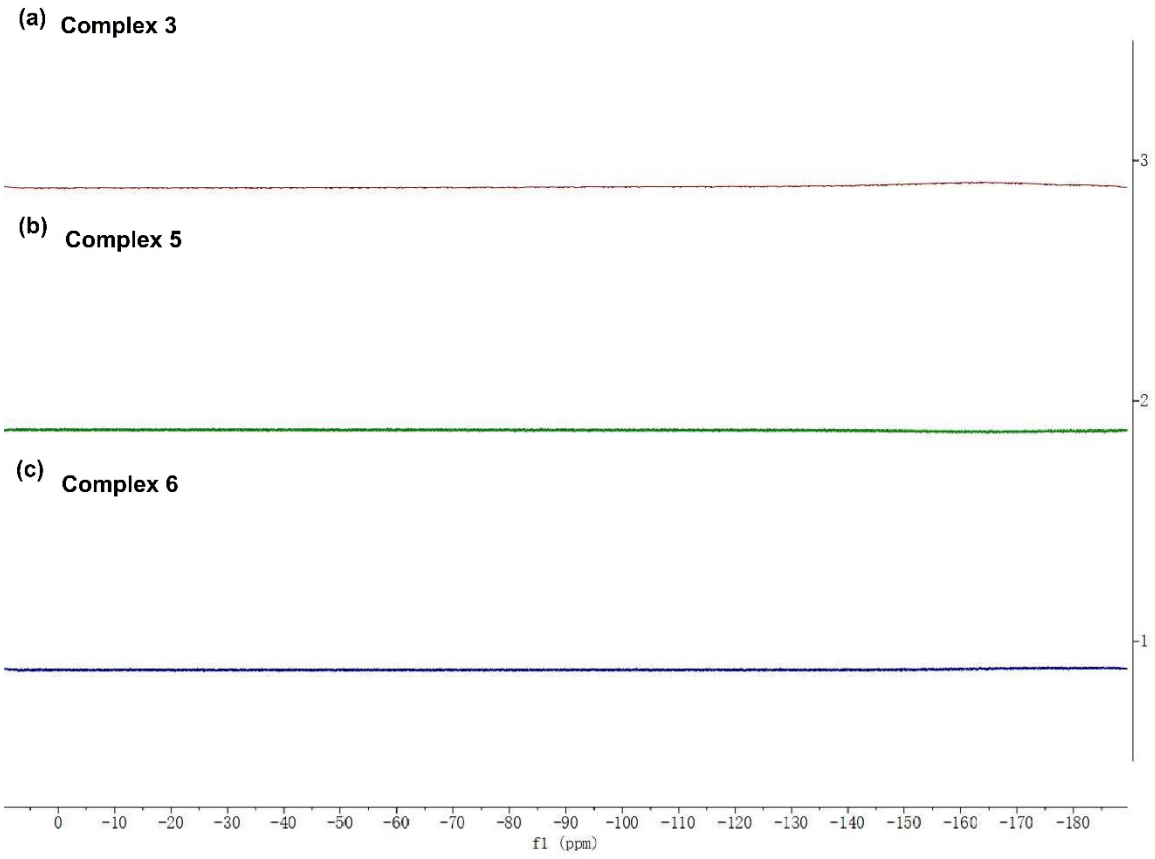


**Figure S 39.** (a) $^{19}$F-NMR spectrum of **3** in MeOD, 400 MHz; (b) $^{19}$F-NMR spectrum of **5** in MeOD, 400 MHz; (c) $^{19}$F-NMR spectrum of **6** in MeOD, 400 MHz.

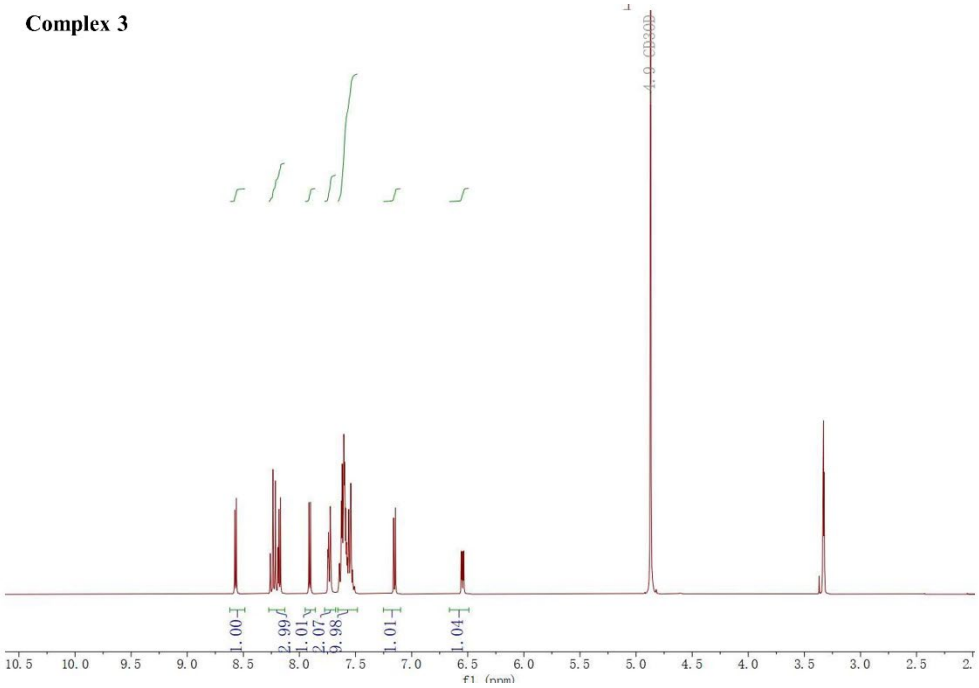

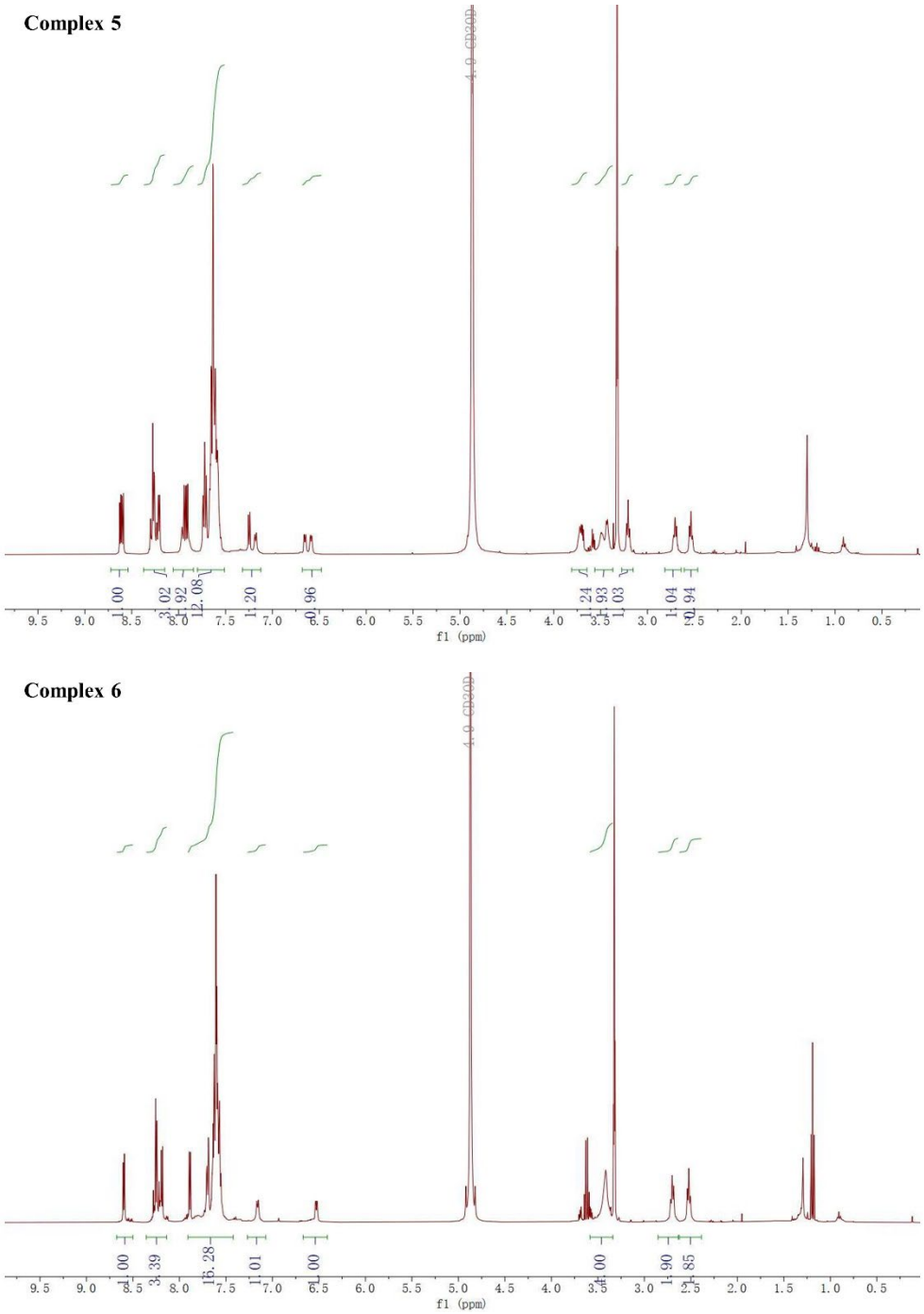


**Figure S 40.** $^{1}$H-NMR spectrum of **3, 5 and 6** with chloride counteranion in MeOD, 400 MHz.

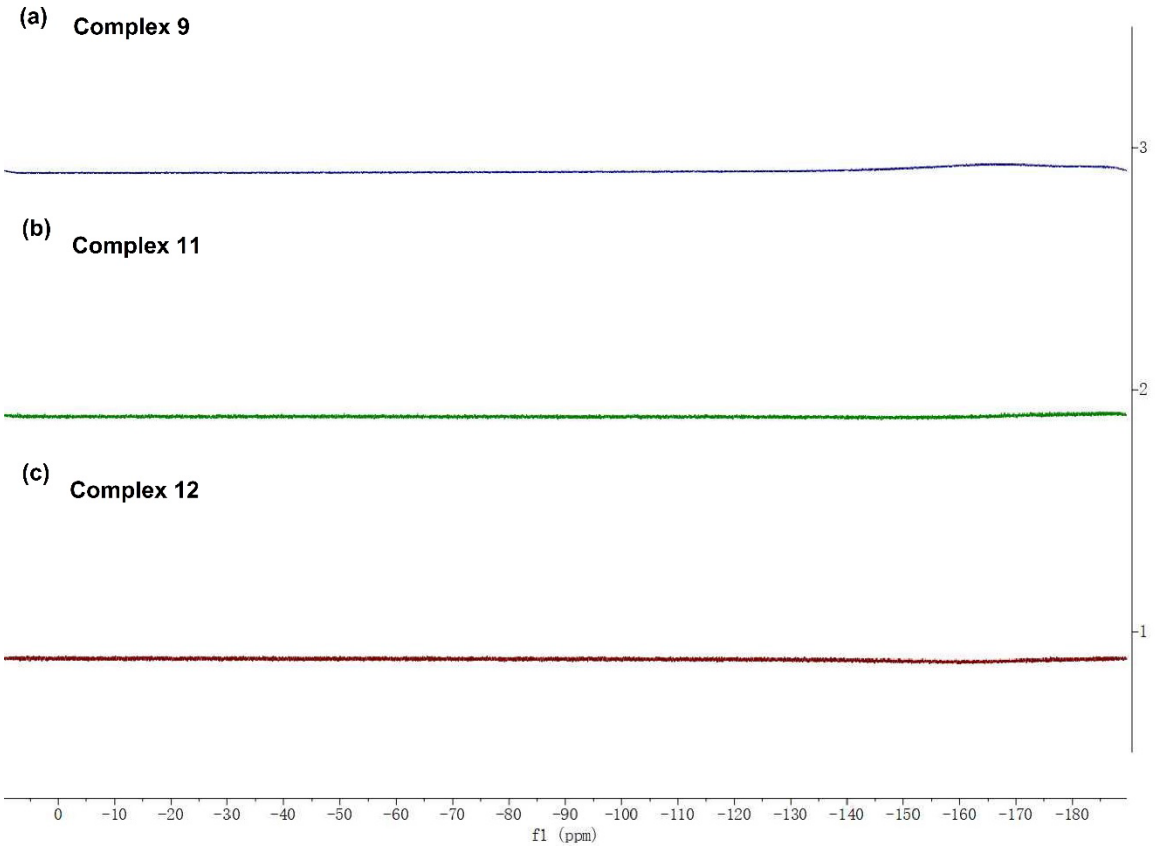


**Figure S 41.** (a) $^{19}$F-NMR spectrum of **9** in MeOD, 400 MHz; (b) $^{19}$F-NMR spectrum of **11** in MeOD, 400 MHz; (c) $^{19}$F-NMR spectrum of **12** in MeOD, 400 MHz.

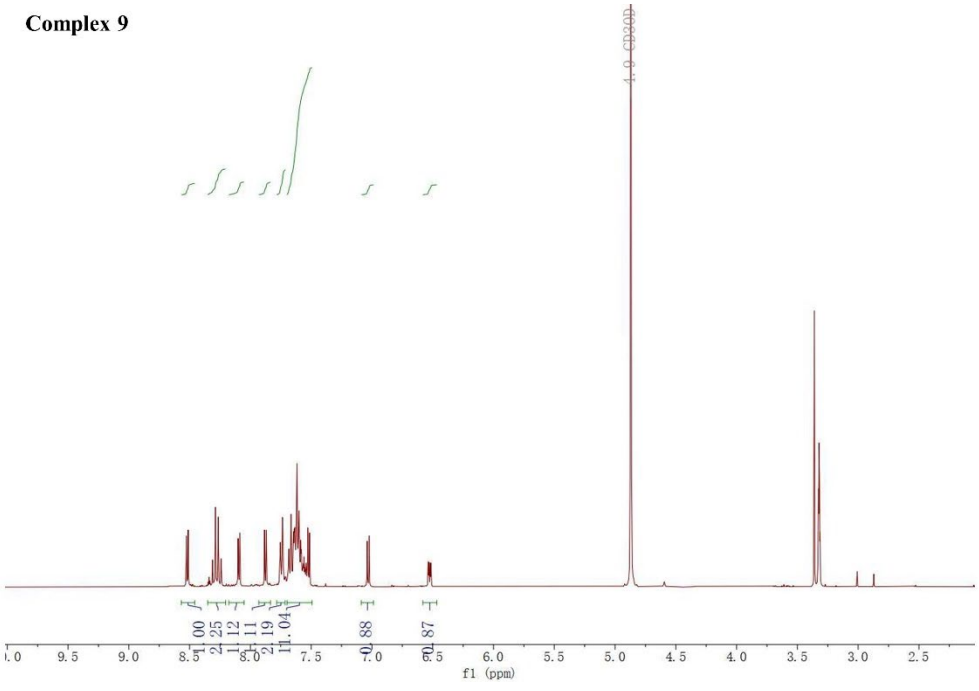

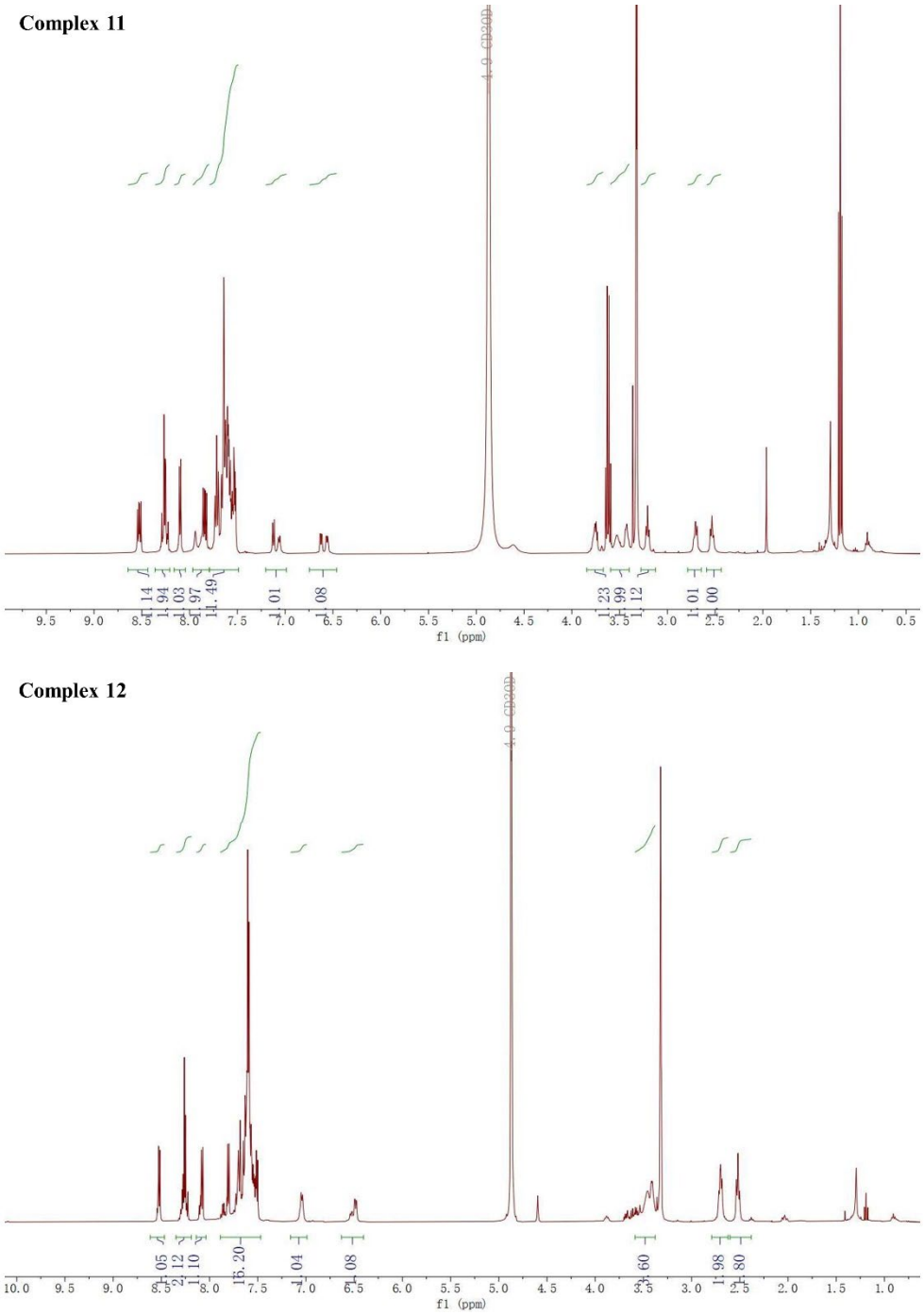


**Figure S 42.** $^{1}$H-NMR spectrum of **9, 11 and 12** with chloride counteranion in MeOD, 400 MHz.

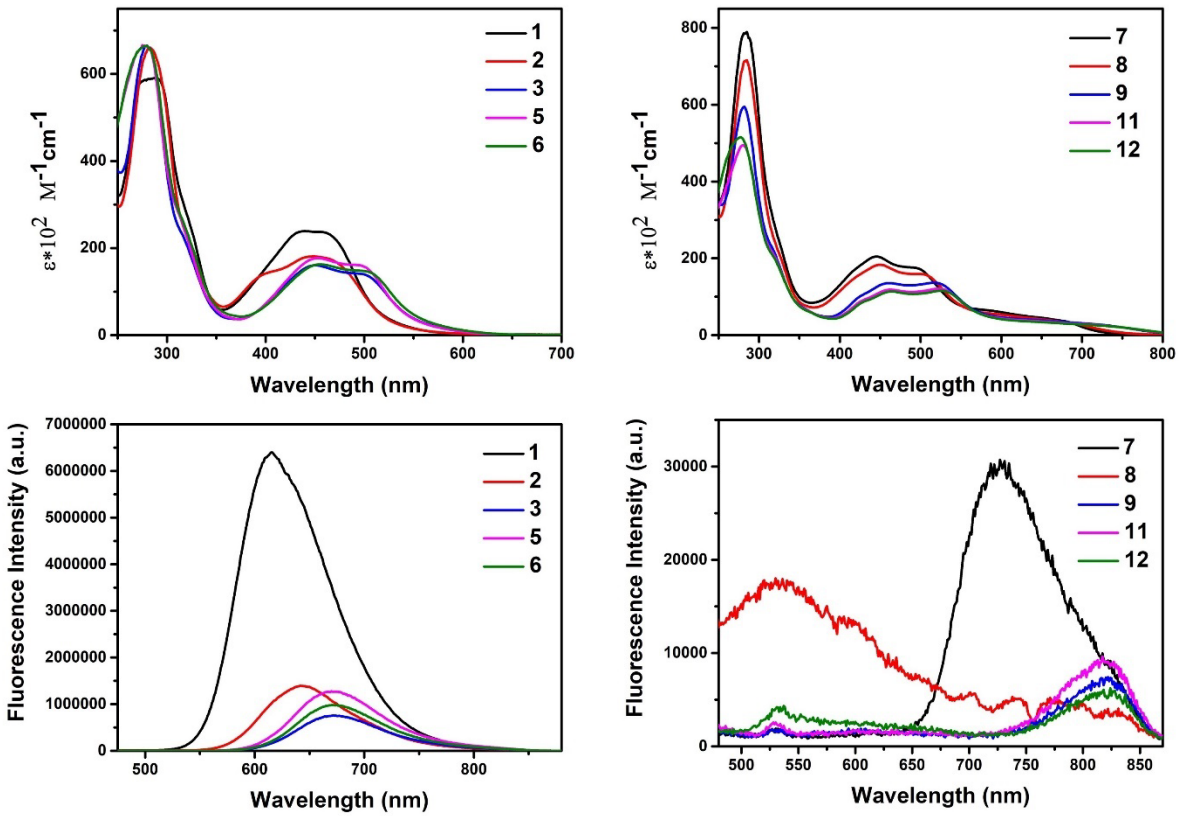


**Figure S 43.** UV-Vis absorption spectra and emission spectra of complexes measured in $H_2O$.a) the UV-Vis spectra of Ru(II) complexes ( 50 μM of complexes **1**, **2**, **3**, **5**, **6**); b) the UV-Vis spectra of Os(II) complexes (complexes **7**, **8**, **9**, **11**, **12**); c) fluorescence spectra of Ru(II) complexes (complexes **1**, **2**, **3**, **5**, **6**), (concentration: 50 μM, excitation:450 nm, slit: 6 nm); d) fluorescence spectra of Os(II) complexes (complexes **7**, **8**, **9**, **11**, **12**), (concentration: 50 μM, excitation:450 nm, slit: 6 nm).

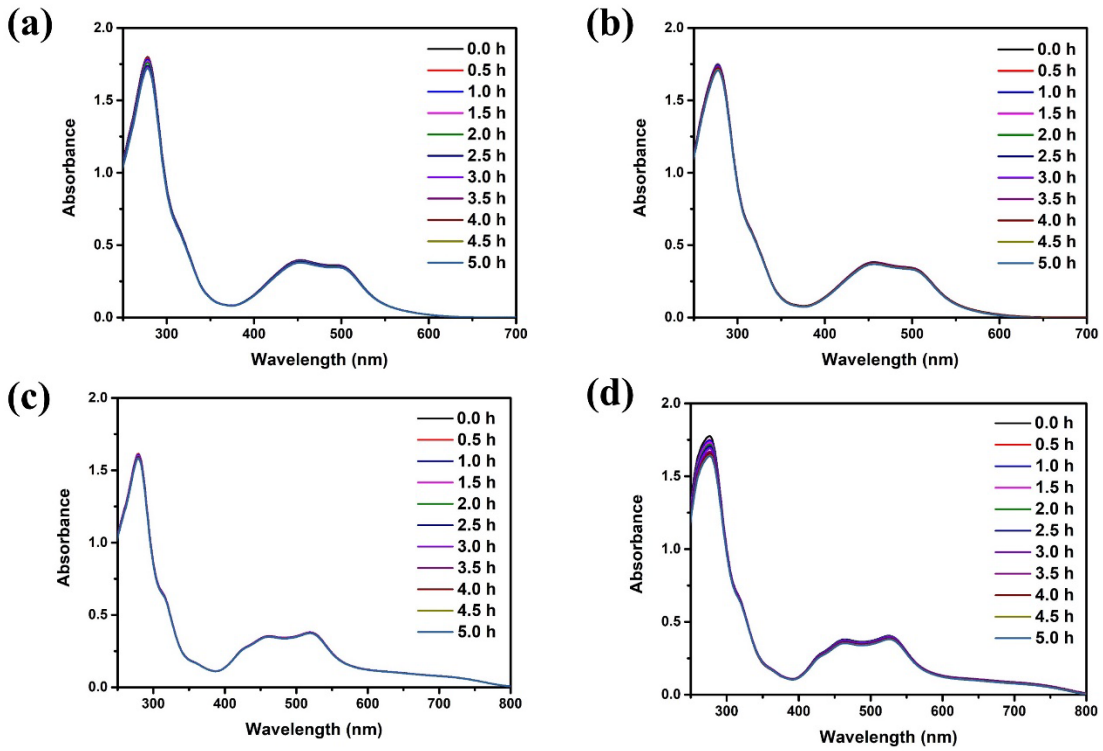


**Figure S 44**. The stability of complexes (50 μM).(a) **5-2PF$_6^-$**, (b) **6-2PF$_6^-$**, (c) **11-2PF$_6^-$** and (d) **12-2PF$_6^-$**.

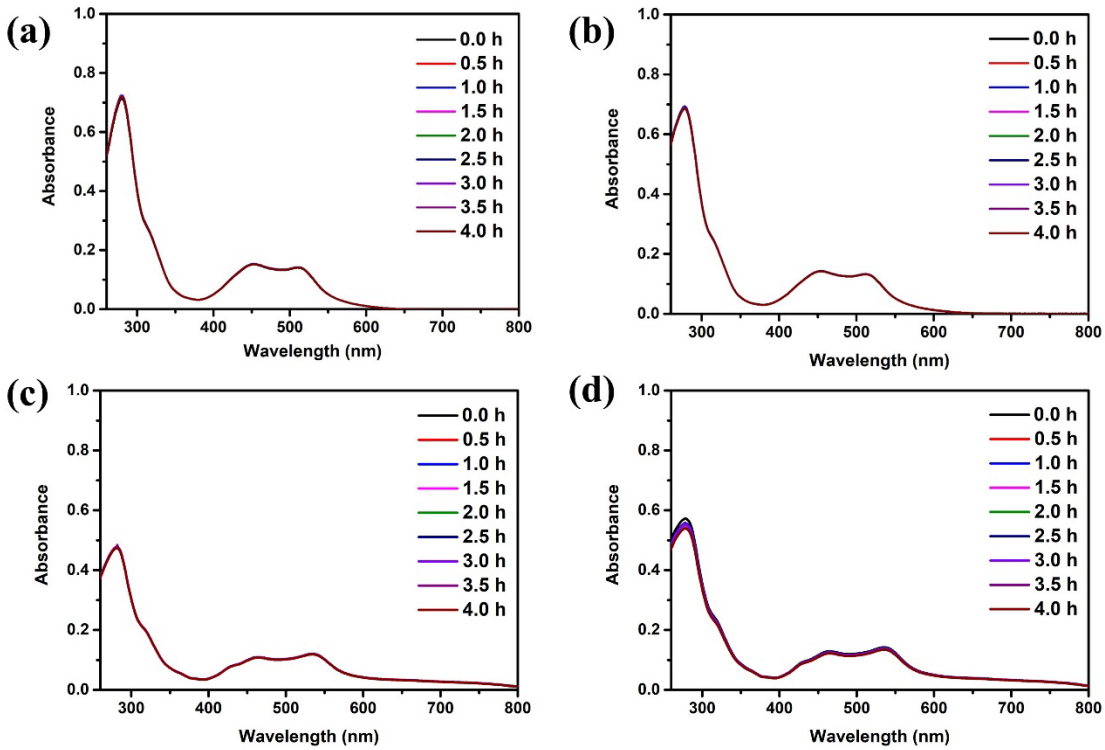


**Figure S 45.** The stability of complexes with $Cl^-$ (10 μM) in 10 mM pH = 7.4Tris-buffer solution in presence of 0.2% Tween-80.(a) **5-2Cl$^-$**, (b) **6-2Cl$^-$**, (c) **11-2Cl$^-$** and (d) **12-2Cl$^-$**.

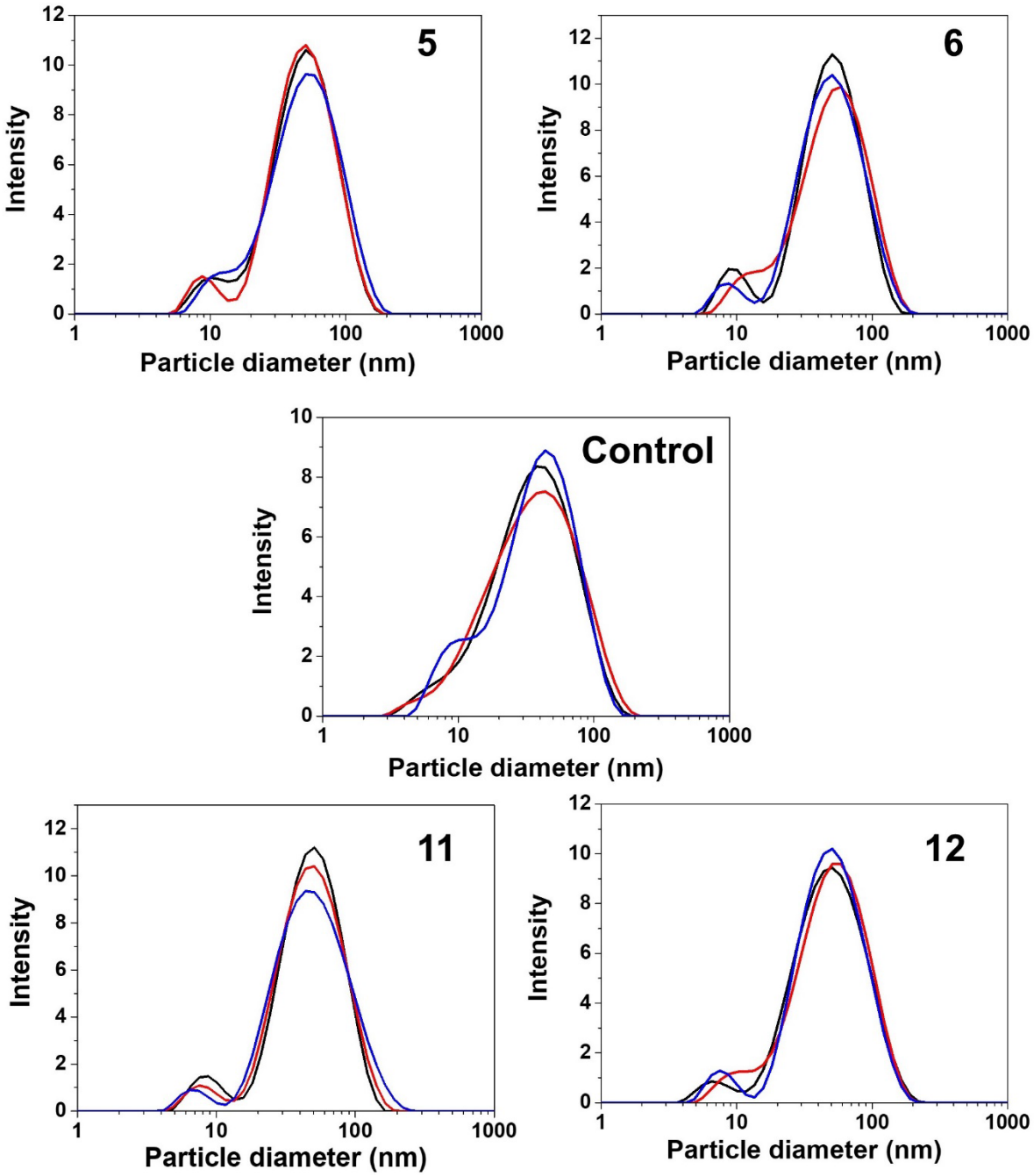


**Figure S 46.** Dynamic light scattering data: particle size distribution by the intensity of control, complexes **5,6** and **11,12** (10 μM) in 10% FBS in PBS.

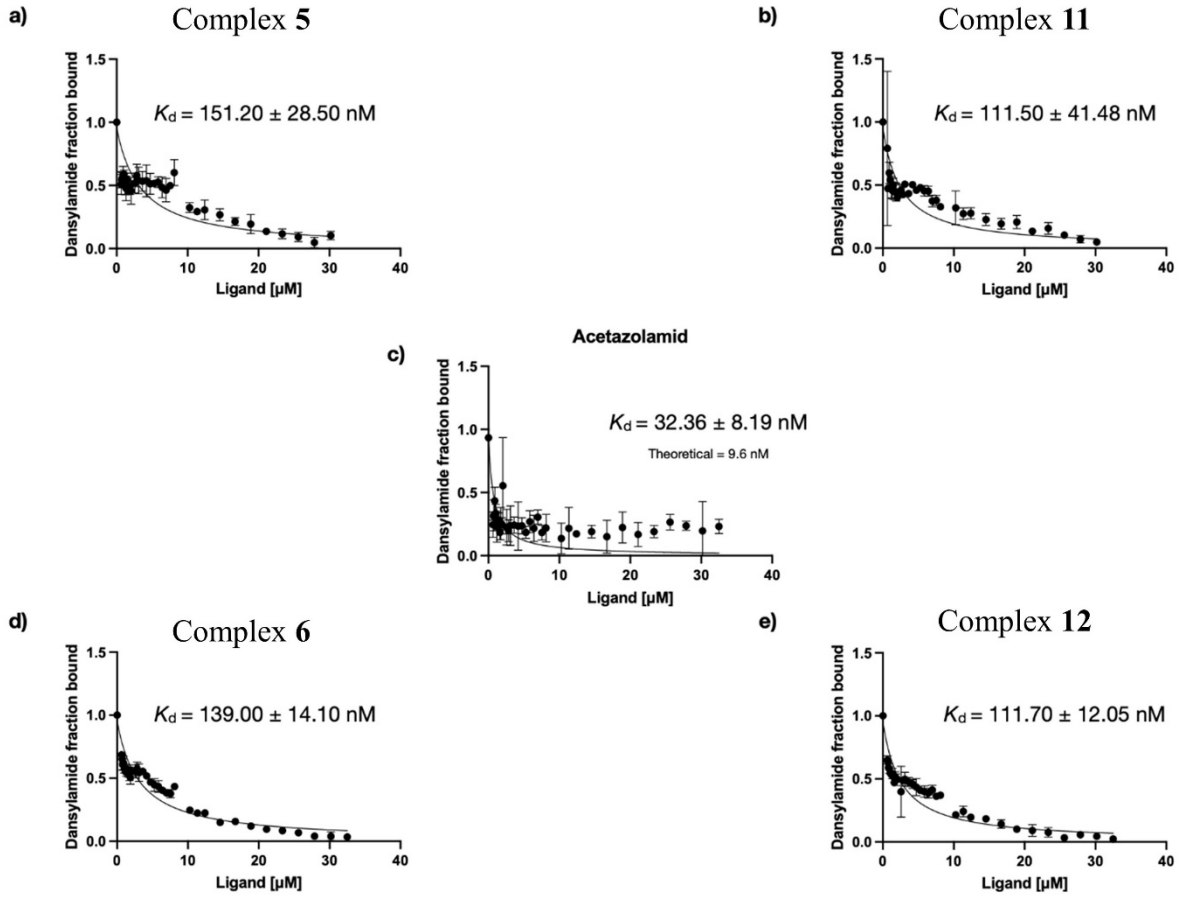


**Figure S 47.** Determination of the dissociation constants for various ligand.

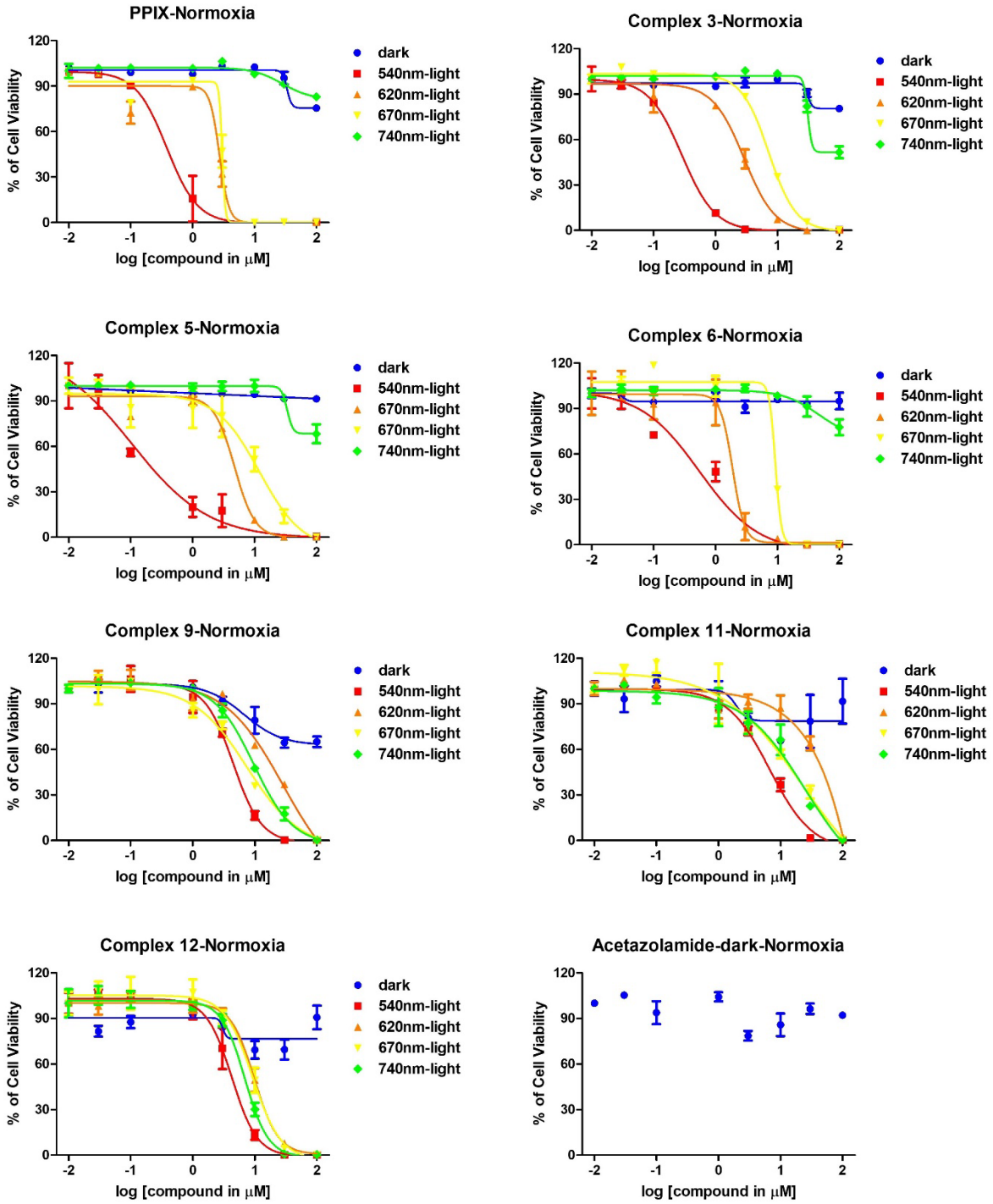


**Figure S 48.** Phototoxicity and cytotoxicity of complexes incubated with A549 cell line in normoxia condition.

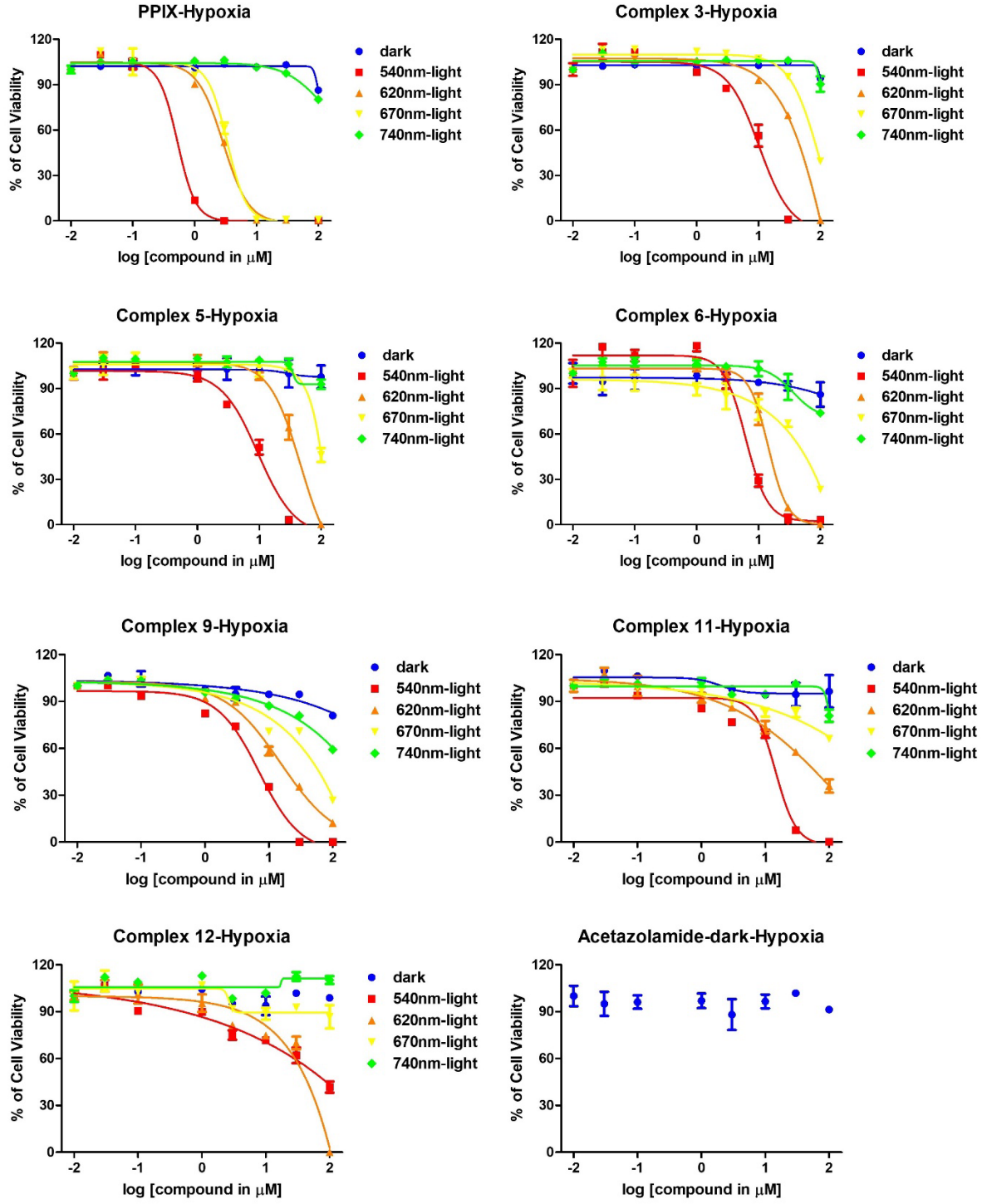


**Figure S 49.** Phototoxicity and cytotoxicity of complexes incubated with A549 cell line in hypoxia condition.

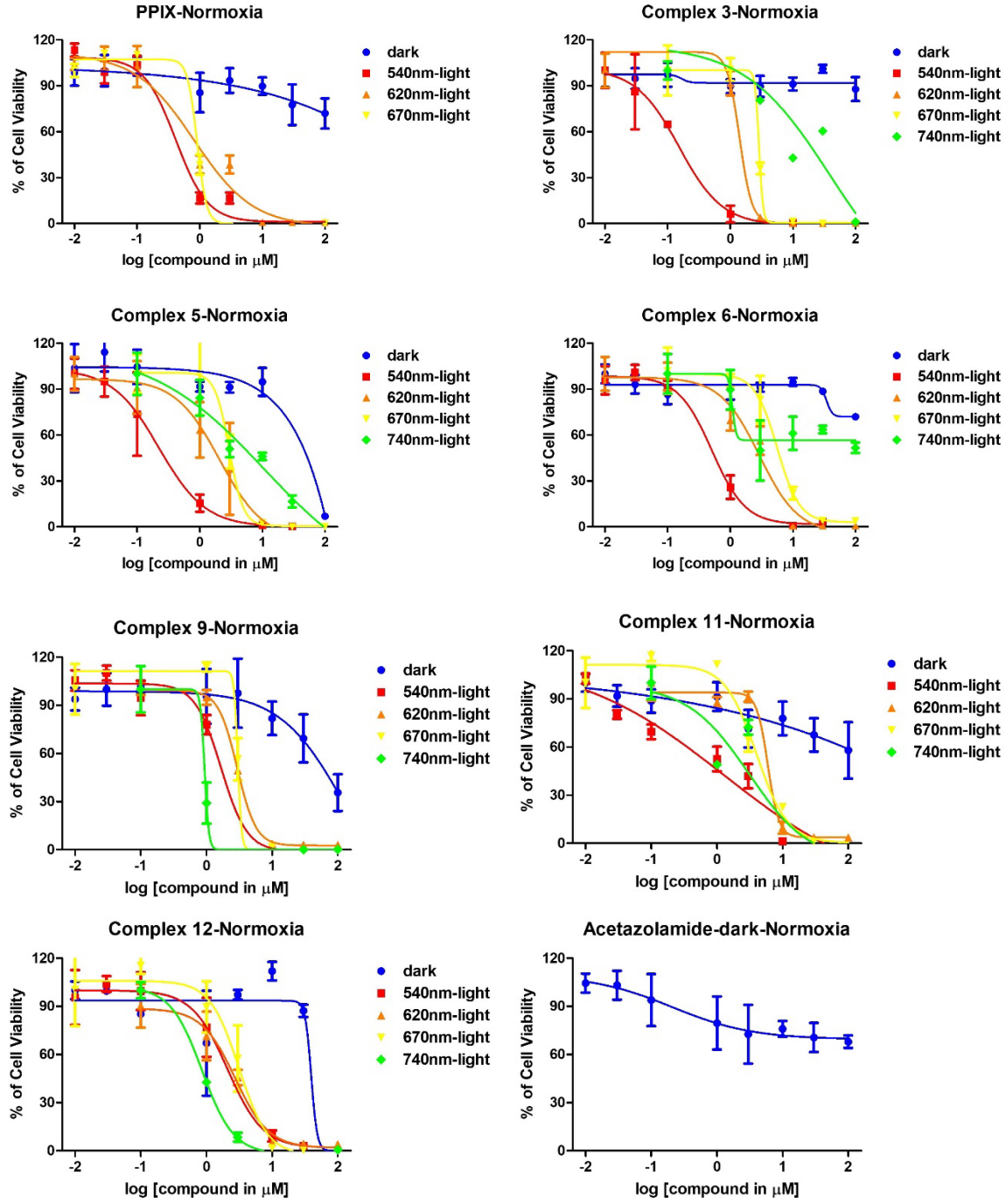


**Figure S 50.** Phototoxicity and cytotoxicity of complexes incubated with MDA-MB-231 cell line in normoxia condition.

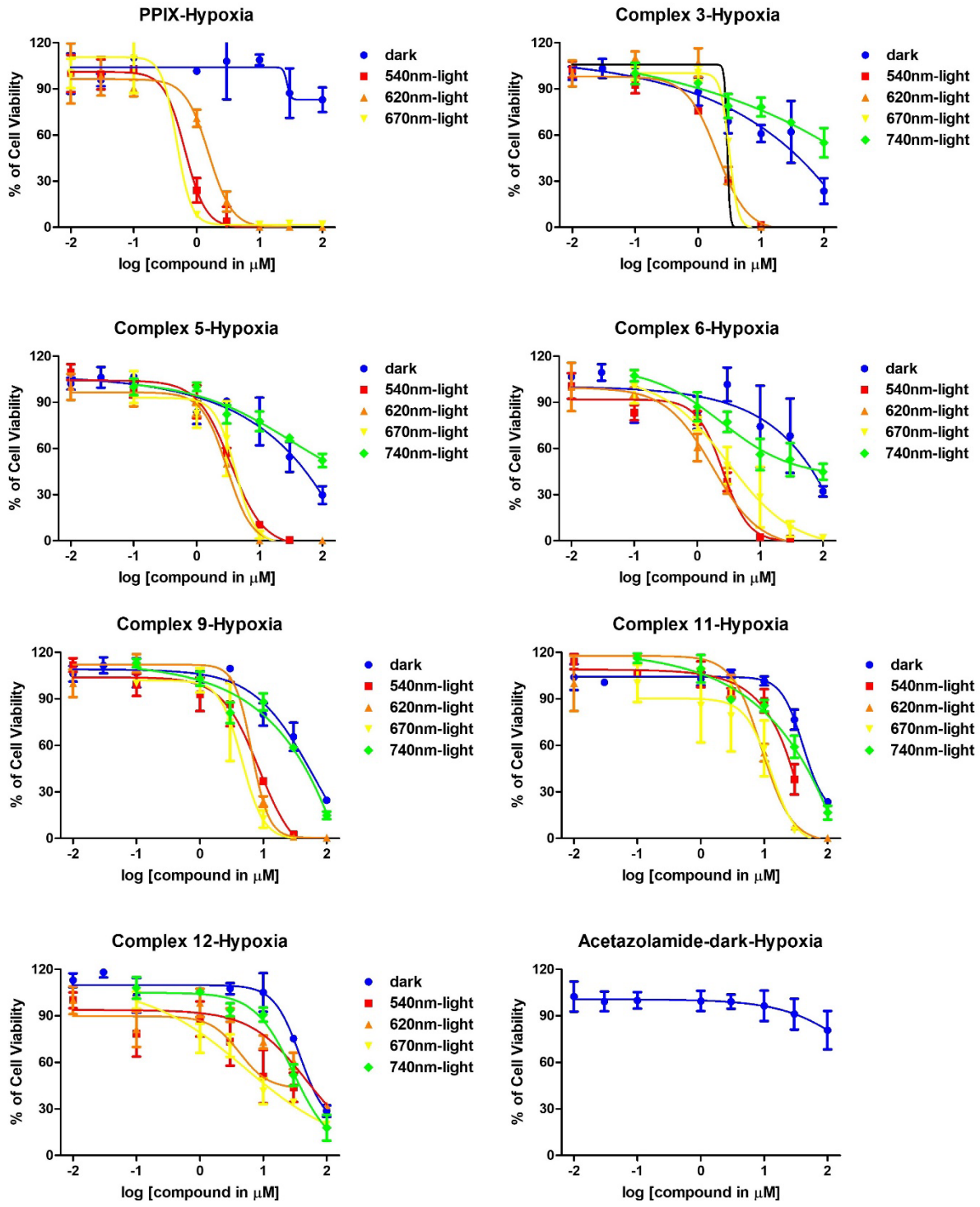


**Figure S 51.** Phototoxicity and cytotoxicity of complexes incubated with MDA-MB-231 cell line in hypoxia condition.

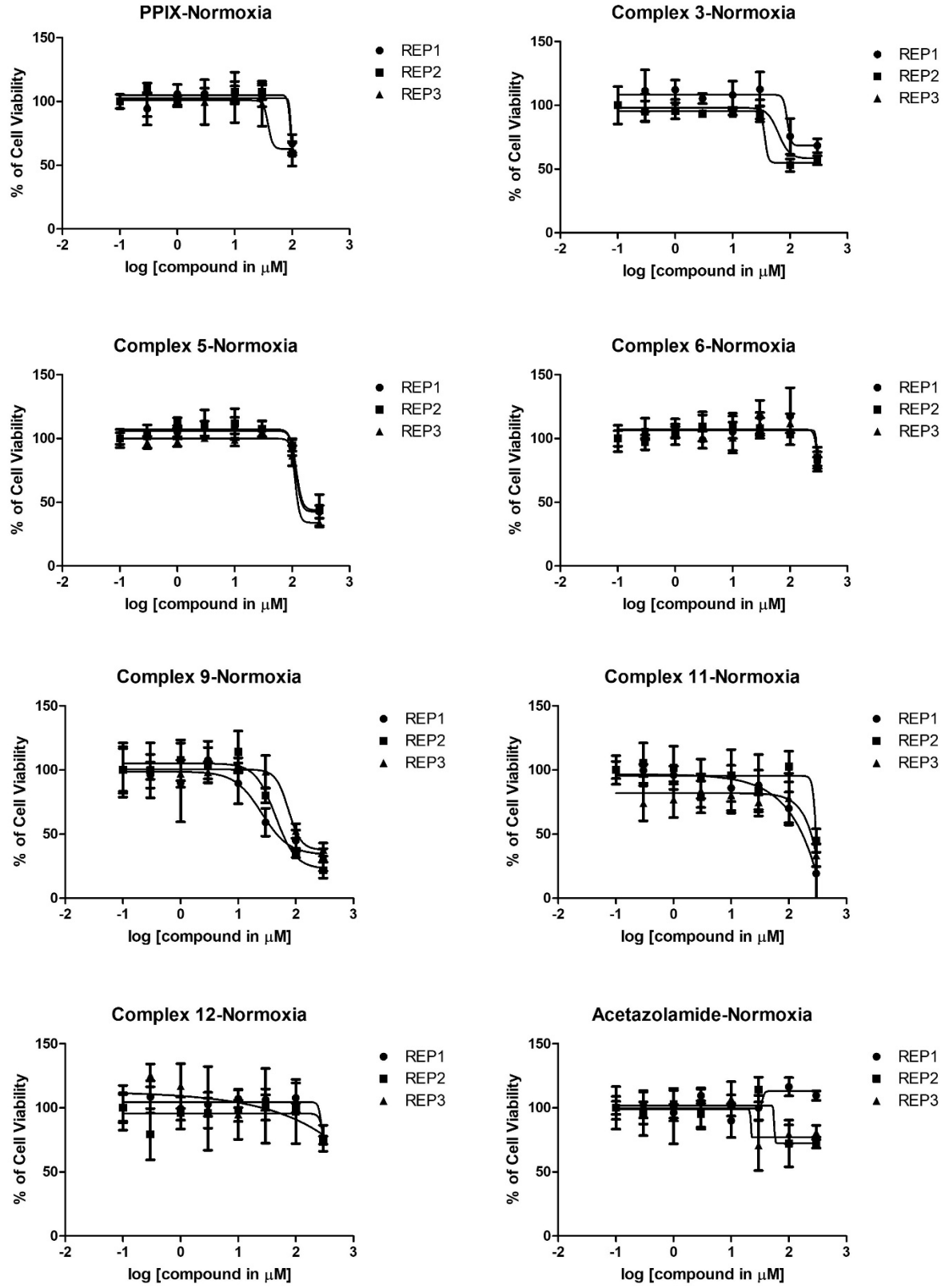


**Figure S 52.** Cytotoxicity of complexes incubated with RPE-1 cell line in normoxia condition.

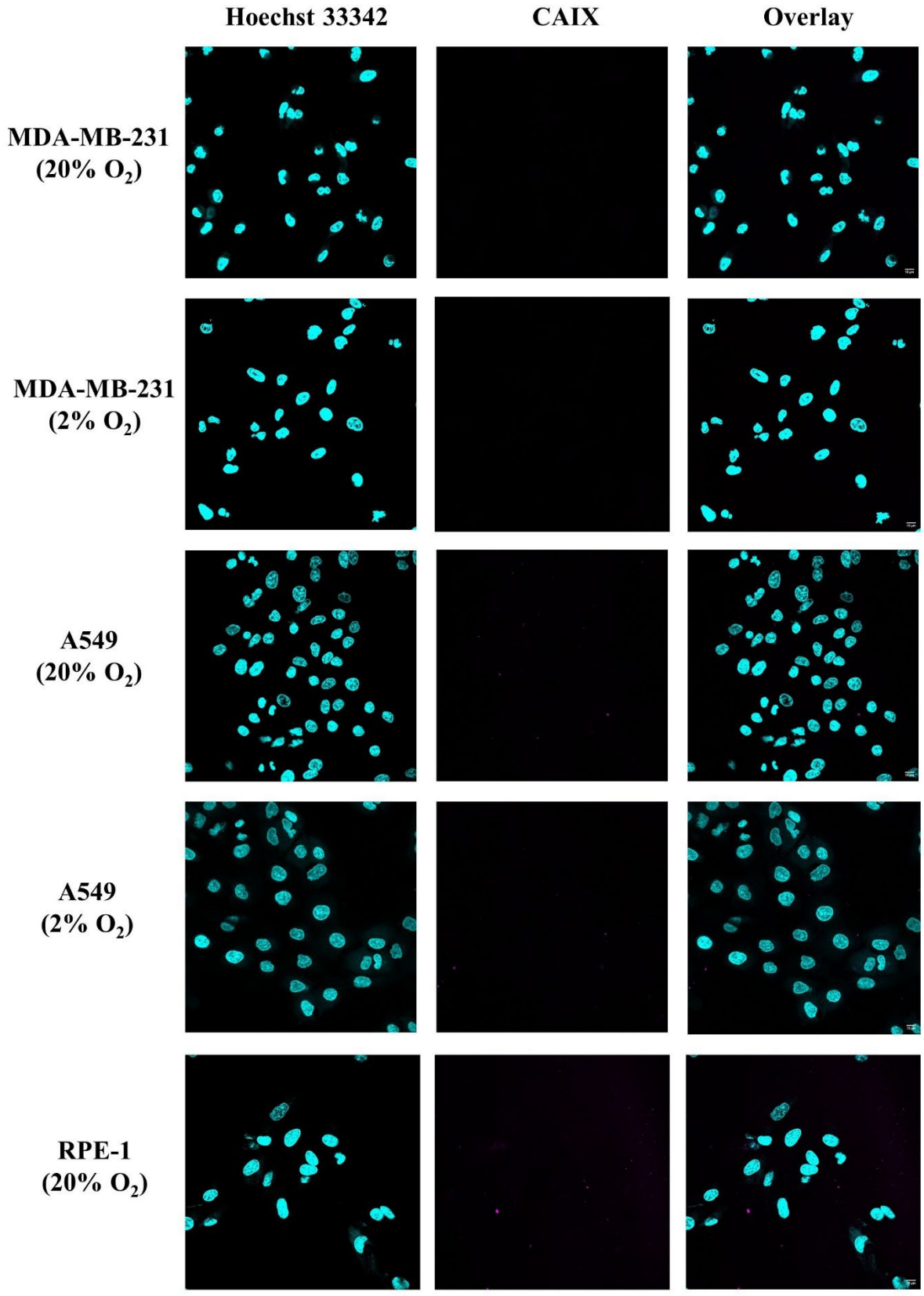


**Figure S 53.** Control experiment for CAIX immunostaining. A549, MDA-MB-231 and RPE1 cells were stained as indicated in the Method but omitting anti-CAIX primary antibody.

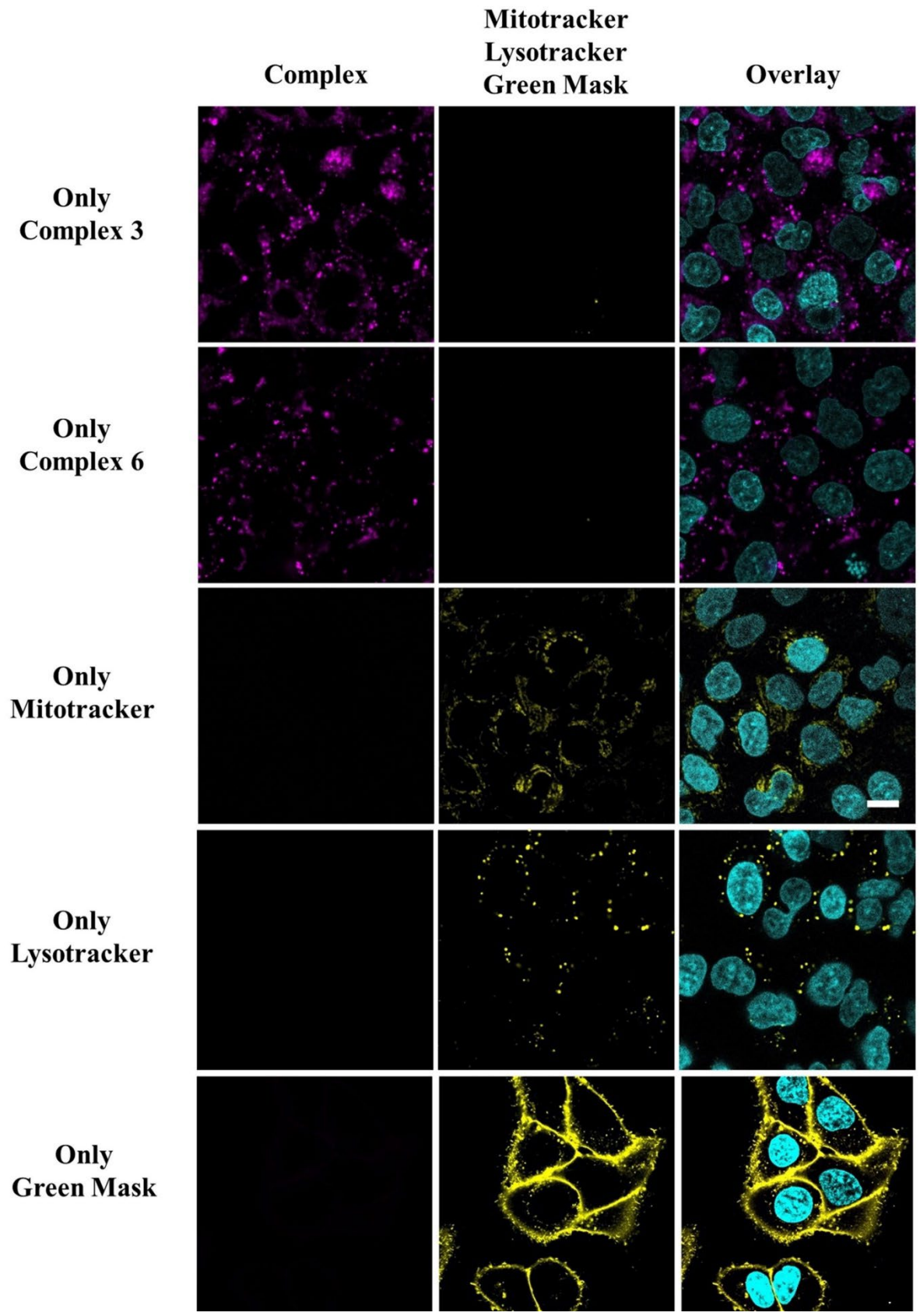


**Figure S 54.** Control experiment for Ru complexes for confocal imaging. A549 cells incubated with only complex **3** (5 μM, 4 h), only complex **6** (5 μM, 4 h), only MitoTracker Green (MTG, 100 nM, 10 min), Lyso Tracker Green (LTG, 100 nM, 40 min) or only Green Mask (100 nM,

10 min). Excitation/Emission wavelengths are 405/420-450 nm (Hoechst), 488/670-800 nm (Complex **3** and Complex **6)**, 488/500-550 nm (Green CellMask, MTG and LTG), respectively. The scale bar is 10 μm.

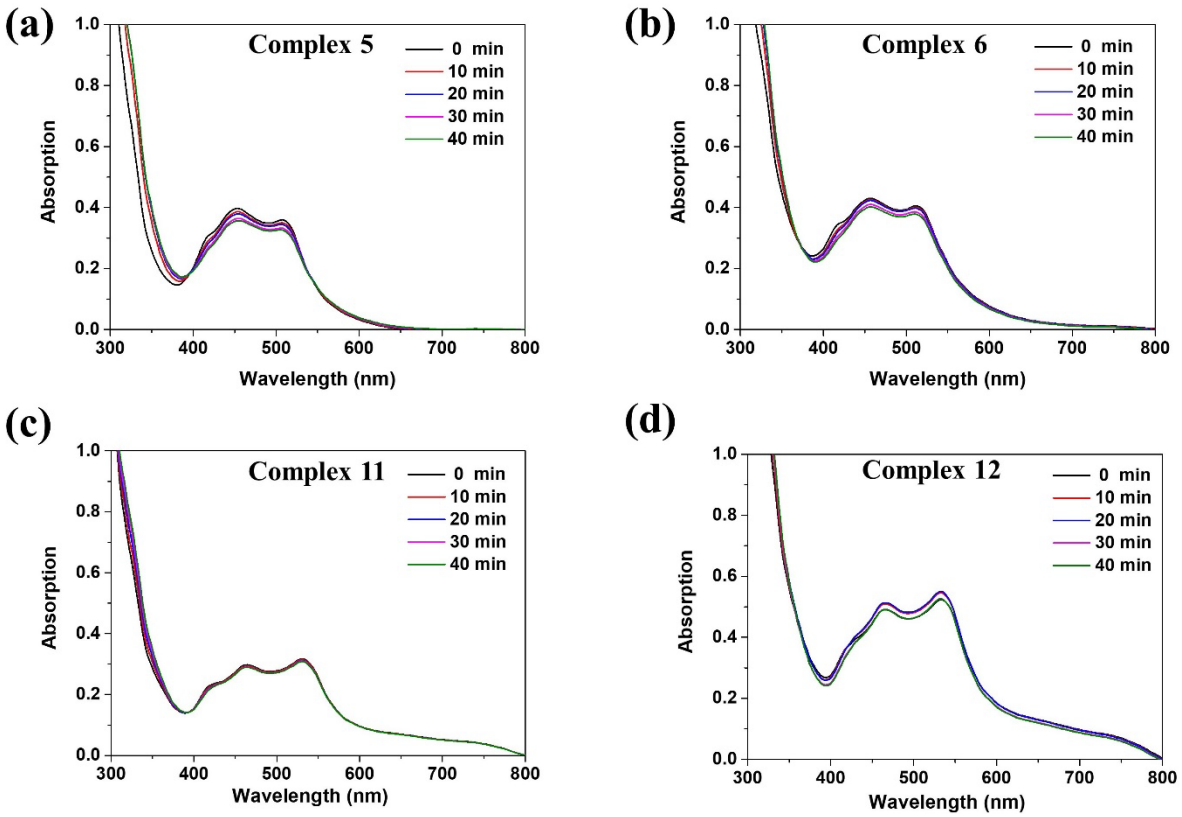


**Figure S 55.** Absorption spectrum changes upon irradiation (540 nm, 9.0 J/cm$^2$) of complexes using 10% FBS in PBS as solvents.

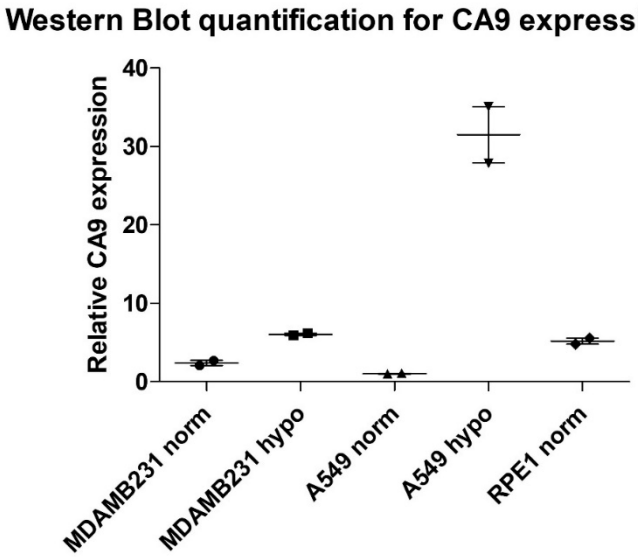


**Figure S 56.** Quantitative measurement of CA expression by Western blot.

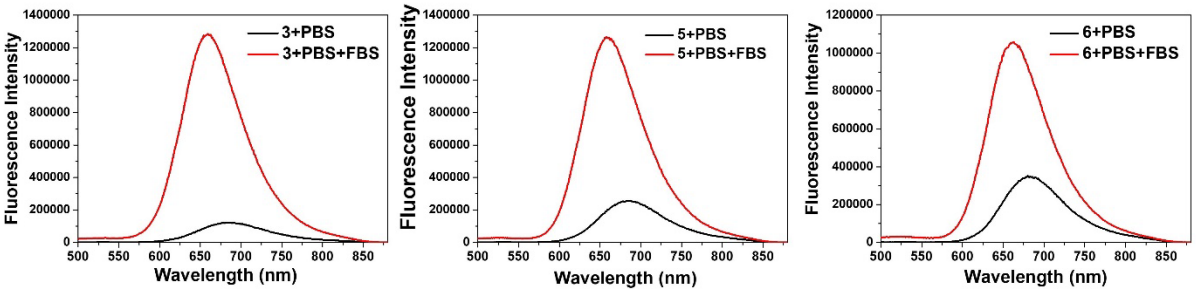


**Figure S 57.** Fluorescence spectra of Ru(II) complexes (complexes **3**, **5**, **6**) in the absence or presence of 10%FBS (concentration: 10 μM, 1% DMSO, excitation: 450 nm, slit: 6 nm).

## 16. References


(1) Sullivan, B. P.; Salmon, D. J.; Meyer, T. J. Mixed Phosphine 2,2'-Bipyridine Complexes of Ruthenium. *Inorg. Chem.* **1978**, *17* (12), 3334–3341. https://doi.org/10.1021/ic50190a006.

(2) Carlson, B.; Phelan, G. D.; Kaminsky, W.; Dalton, L.; Jiang, X.; Liu, S.; Jen, A. K.-Y. Divalent Osmium Complexes: Synthesis, Characterization, Strong Red Phosphorescence, and Electrophosphorescence. *J. Am. Chem. Soc.* **2002**, *124* (47), 14162–14172. https://doi.org/10.1021/ja0176705.

(3) Mongelli, M. T.; Brewer, K. J. Synthesis and Study of the Light Absorbing, Redox and Photophysical Properties of Ru(II) and Os(II) Complexes of 4,7-Diphenyl-1,10-Phenanthroline Containing the Polyazine Bridging Ligand 2,3-Bis(2-Pyridyl)Pyrazine. *Inorganic Chemistry Communications* **2006**, *9* (9), 877–881. https://doi.org/10.1016/j.inoche.2006.04.022.

(4) Notaro, A.; Jakubaszek, M.; Rotthowe, N.; Maschietto, F.; Vinck, R.; Felder, P. S.; Goud, B.; Tharaud, M.; Ciofini, I.; Bedioui, F.; Winter, R. F.; Gasser, G. Increasing the Cytotoxicity of Ru(II) Polypyridyl Complexes by Tuning the Electronic Structure of Dioxo Ligands. *J. Am. Chem. Soc.* **2020**, *142* (13), 6066–6084. https://doi.org/10.1021/jacs.9b12464.

(5) Vinck, R.; Karges, J.; Tharaud, M.; Cariou, K.; Gasser, G. Physical, Spectroscopic, and Biological Properties of Ruthenium and Osmium Photosensitizers Bearing Diversely Substituted 4,4′-Di(Styryl)-2,2′-Bipyridine Ligands. *Dalton Trans.* **2021**, *50* (41), 14629–14639. https://doi.org/10.1039/D1DT02083H.

(6) Su, X.; Wang, W.; Cao, Q.; Zhang, H.; Liu, B.; Ling, Y.; Zhou, X.; Mao, Z. A Carbonic Anhydrase IX (CAIX)-Anchored Rhenium(I) Photosensitizer Evokes Pyroptosis for Enhanced Anti-Tumor Immunity. *Angew Chem Int Ed* **2022**, *61* (8), e202115800. https://doi.org/10.1002/anie.202115800.

(7) Ishida, H.; Tobita, S.; Hasegawa, Y.; Katoh, R.; Nozaki, K. Recent Advances in Instrumentation for Absolute Emission Quantum Yield Measurements. *Coordination Chemistry Reviews* **2010**, *254* (21–22), 2449–2458. https://doi.org/10.1016/j.ccr.2010.04.006.

(8) Tanielian, C.; Wolff, C.; Esch, M. Singlet Oxygen Production in Water: Aggregation and Charge-Transfer Effects. *J. Phys. Chem.* **1996**, *100* (16), 6555–6560. https://doi.org/10.1021/jp952107s.
(9) Kępczyński, M.; Pandian, R. P.; Smith, K. M.; Ehrenberg, B. Do Liposome-Binding Constants of Porphyrins Correlate with Their Measured and Predicted Partitioning Between Octanol and Water?¶. *Photochemistry and Photobiology* **2007**, *76* (2), 127–134. https://doi.org/10.1562/0031-8655(2002)0760127DLBCOP2.0.CO2.
(10) Ahmedi, R.; Lanez, T. Experimental Partition Determination of Octanol-Water Coefficients of Ferrocene Derivatives Using Square Wave Voltammetry Techniques. *J. Fundam and Appl Sci.* **2018**, *10* (1), 308. https://doi.org/10.4314/jfas.v10i1.23.
(11) Wang, S. C.; Zamble, D. B. Fluorescence Analysis of Sulfonamide Binding to Carbonic Anhydrase. *Biochem. Mol. Biol. Educ.* **2006**, *34* (5), 364–368. https://doi.org/10.1002/bmb.2006.494034052656.
(12) Ansar Ahmed, S.; Gogal, R. M.; Walsh, J. E. A New Rapid and Simple Non-Radioactive Assay to Monitor and Determine the Proliferation of Lymphocytes: An Alternative to [3H]Thymidine Incorporation Assay. *Journal of Immunological Methods* **1994**, *170* (2), 211–224. https://doi.org/10.1016/0022-1759(94)90396-4.